

Dynamic stability of electric power grids: Tracking the interplay of the network structure, transmission losses, and voltage dynamics

Cite as: Chaos **32**, 053117 (2022); <https://doi.org/10.1063/5.0082712>

Submitted: 17 December 2021 • Accepted: 07 April 2022 • Published Online: 10 May 2022

 Philipp C. Böttcher,  Dirk Witthaut and  Leonardo Rydin Gorjão



[View Online](#)



[Export Citation](#)



[CrossMark](#)

APL Machine Learning

Open, quality research for the networking communities

COMING SOON

[LEARN MORE](#)



Dynamic stability of electric power grids: Tracking the interplay of the network structure, transmission losses, and voltage dynamics

Cite as: Chaos 32, 053117 (2022); doi: 10.1063/5.0082712

Submitted: 17 December 2021 · Accepted: 7 April 2022 ·

Published Online: 10 May 2022




View Online



Export Citation



CrossMark

Philipp C. Böttcher,^{1,2,a)}  Dirk Witthaut,^{1,3,b)}  and Leonardo Rydin Gorjão^{1,2,3,c)} 

AFFILIATIONS

¹Forschungszentrum Jülich, Institute for Energy and Climate Research—Systems Analysis and Technology Evaluation (IEK-STE), 52428 Jülich, Germany

²German Aerospace Center (DLR), Institute of Networked Energy Systems, 26129 Oldenburg, Germany

³Institute for Theoretical Physics, University of Cologne, 50937 Köln, Germany

^{a)}Author to whom correspondence should be addressed: p.boettcher@fz-juelich.de

^{b)}Electronic mail: d.witthaut@fz-juelich.de

^{c)}Electronic mail: leonardo.rydin@gmail.com

ABSTRACT

Dynamic stability is imperative for the operation of the electric power system. This article provides analytical results and effective stability criteria focusing on the interplay of network structures and the local dynamics of synchronous machines. The results are based on an extensive linear stability analysis of the third-order model for synchronous machines, comprising the classical power-swing equations and the voltage dynamics. The article addresses the impact of Ohmic losses, which are important in distribution and microgrids but often neglected in analytical studies. We compute the shift of the stability boundaries to leading order, and thus provide a detailed qualitative picture of the impact of Ohmic losses. A subsequent numerical study of the criteria is presented, without and with resistive terms, to test how tight the derived analytical results are.

Published under an exclusive license by AIP Publishing. <https://doi.org/10.1063/5.0082712>

The secure supply of electric power relies on the stable, coordinated operation of thousands of electric machines connected via the power grid. At the transmission grid level, machines run synchronously with fixed voltage magnitudes and stationary relative phase angles defining a stationary state. The ongoing introduction of renewable power systems poses several challenges to the stability of the system, as situations with highly loaded lines and temporal fluctuations increase considerably. This trend takes place in both the transmission grid at high voltages, as well as in distribution grids and microgrids at medium and low voltages. This article contributes to the understanding of dynamical stability of electric power systems and provides a detailed analysis of the third-order model for synchronous generators, which includes the transient dynamics of voltage magnitudes. Special emphasis is laid on the impact of Ohmic losses in the transmission of power, which are often neglected in analytical treatments of power system stability. The analytical results thus find applicability on all size scales of power grids, from transmission grids

to isolated microgrids, for openly tackling systems with losses in a rigorous analytical manner. Furthermore, the results are independent of the network construction and entail explicit criteria for the connectivity of the power grid and the physical requirements needed to ensure stability in the presence of resistive terms.

I. INTRODUCTION

The unwavering operation of the electric power systems is vital to our daily life and the continued function of modern societies as a whole. Thus, an improved understanding of the electrical system's dynamic properties is especially relevant at present, as more renewable energies enter the electric power grid systems.^{1,2} One of the key elements at play is the relative reduction of inertial mass in power systems due to the penetration of renewable generation, which can lead to large dynamic responses to

disturbances.^{3–6} An expected higher grid load and stronger fluctuating generation by wind and solar resources may further threaten the dynamic stability.^{7–9} Additionally, conventional power generation typically involves large rotating masses that offer stabilizing inertia.¹⁰

Power grids can be of various scales, spanning from entire continents to single islands. Recently, the concept of microgrids has emerged:^{11–13} partially independent power grids in smaller environments that are coupled to a main power grid. These power grids operate at lower voltages than conventional transmission grids and are capable of producing their own power, consequently working partially independently from an overlying power grid.^{14,15} Microgrids embedded in power grids are still ruled by a common understanding of fixed nominal reference frequency, e.g., 50 Hz in Europe, among many other stability criteria.^{16,17}

Analytical approaches to stability in power grid systems are a difficult task and generally rely on model simplifications to keep the problem tractable.^{18–24} The most common simplification to make stability problems mathematically tractable is the assumption of having lossless systems.^{25,26} Various such studies with complex dynamical models exist, cf. Schiffer *et al.*^{27–29} and Dörfler *et al.*,^{30,31} yet results are scarce for extended networks including resistive terms, given the difficulty of tackling dissipative systems mathematically. The problem of losses in power grid systems is often tackled using extensive numerical simulations.^{32,33}

This article puts forth a set of mathematical stability criteria for power grids based on the third-order model for synchronous generators.^{34–39} The criteria can be employed for various scales of power grids—for both transmission and distribution grids—evidencing the limitations entailed by the existence of resistive terms on the operability of power grid systems. In particular, this article undertakes the task of intertwining results for graph theory with the characteristics of the power grid construction and their physical properties,^{40,41} extending a previous article on lossless power grids.⁴²

The article is structured in the following manner: Sec. II introduces the basic dynamical model studied in this paper. In this work, we present an analysis of the third-order model, comprising transient voltage dynamics and considering extended grids with complex topology and resistive losses. Section III tackles the linear stability analysis of the equations of motion, a reduction of the problem to a matrix formulation, and develops a mathematical apparatus to unveil sufficient criteria for stability in a general sense. Section IV introduces the two main lemmata of the article from which various stability criteria are derived. Lemma 2 covers solely lossless grids and Lemma 4 extends the results to the case of lossy transmission up to leading order in the losses in the system, which is drawn from perturbation theory. In Sec. V, the developed concepts are utilized to derive analytical stability conditions for both lossless and lossy systems, presenting criteria for stability not only for the power-angle and the voltage dynamics but also for a mixed type of instabilities. These results also represent a direct link to graph-theoretical measures. Section VI comprises a set of numerical studies on model systems to check how tight the derived bounds are. The conclusions follow subsequently in Sec. VII.

II. MODELING SCALE-INDEPENDENT NETWORK-BASED POWER GRIDS

A. Third-order model for synchronous generators

The third-order model for synchronous machines, denoted as a one or q axis model, describes the transient dynamics of coupled synchronous machines.^{10,32,33} It embodies the power or rotor angle $\delta(t)$, relative to the power grid reference frame, the angular frequency $\omega(t) = \dot{\delta}(t)$, in a co-rotating reference frame rotating with the reference frequency Ω , and the transient voltage $E_q(t)$, in the q direction of a co-rotating frame of reference of each machine in the system. It excludes sub-transient effects, i.e., higher-order effects, and assumes that the transient voltage E_d in the d direction of the co-rotating frame vanishes.

Sub-transient effects play a small role, especially in the case of studying power grids in the vicinity of the steady state.⁴³ The truncation of the transient voltage E_d in the d axis is imposed out of necessity to have an analytically tractable model. Still, the resulting dynamical system is rather complex such that analytical results are scarce and mostly restricted to lossless power grids. Hence, the scope of the analysis here is twofold: to present the details of tackling stability of the rotor angle and voltage systems, while not shunning away from complex network topologies and considering Ohmic losses explicitly.

The equations of motion for one generator are given by¹⁰

$$\begin{aligned}\dot{\delta} &= \omega, \\ M\dot{\omega} &= -D\omega + P^m - P^{\text{el}}, \\ T\dot{E} &= E^f - E + (X - X')I,\end{aligned}\quad (1)$$

where henceforth $E \equiv E_q$ denotes solely the voltage along the q axis, and the dot denotes the differentiation with respect to time. Furthermore, P^m denotes the effective mechanical input power of the machine, E^f denotes the internal voltage or field flux, and P^{el} denotes the electrical power out-flow. The parameters M and D are the inertia and damping of the mechanical motion and T is the relaxation time of the transient voltage dynamics. The voltage dynamics further depend on the difference of the static reactance X and transient reactance X' along the d axis, where $X - X' > 0$, in general, and the current I along the d axis.

The active electrical power P_j^{el} exchanged with the power grid, and the current I_j at the j th machine read³⁴

$$\begin{aligned}P_j^{\text{el}} &= \sum_{\ell=1}^N E_j E_{\ell} [B_{j,\ell} \sin(\delta_j - \delta_{\ell}) + G_{j,\ell} \cos(\delta_j - \delta_{\ell})], \\ I_j &= \sum_{\ell=1}^N E_{\ell} [B_{j,\ell} \cos(\delta_j - \delta_{\ell}) - G_{j,\ell} \sin(\delta_j - \delta_{\ell})],\end{aligned}\quad (2)$$

where E_j and δ_j are the transient voltage and the rotor angle of the j th machine, respectively. The parameters $G_{j,\ell}$ and $B_{j,\ell}$ denote the real and imaginary parts of the nodal admittance matrix and encode the network structure, respectively. Generally, $B_{j,\ell} > 0$ and $G_{j,\ell} < 0$ for all $j \neq \ell$. This article is especially concerned with the role of Ohmic losses, which are described by the real parts of the nodal

admittance matrix $G_{j,\ell}$. All quantities are usually made dimensionless using appropriate scaled units referred to as the “pu system” or “per unit system.”¹⁰

Load nodes are typically described by constant impedances to the ground. These passive nodes can be eliminated from the network equations via Kron reduction such that only generator nodes have to be considered explicit.^{44,45} The remaining nodes are then connected by an effective network that differs considerably from the physical one. For instance, the reduced network is typically fully connected.

The equations of motion (1) for the j th synchronous machine, in a system with N machines, take the form^{34,36,46}

$$\begin{aligned}\dot{\delta}_j &= \omega_j, \\ M_j \dot{\omega}_j &= P_j^m - D_j \omega_j - \sum_{\ell=1}^N E_j E_\ell [B_{j,\ell} \sin(\delta_j - \delta_\ell) + G_{j,\ell} \cos(\delta_j - \delta_\ell)], \\ T_j \dot{E}_j &= E_j^f - E_j + (X_j - X_j') \sum_{\ell=1}^N E_\ell \\ &\quad \times [B_{j,\ell} \cos(\delta_j - \delta_\ell) - G_{j,\ell} \sin(\delta_j - \delta_\ell)].\end{aligned}\quad (3)$$

Most analytical studies so far neglected, under reasonable assumptions, the line losses of the power grid structure. The terms proportional to $G_{j,\ell}$ are assumed to be negligible in comparison with the terms proportional to $B_{j,\ell}$. Such arguments are reasonable for the high-voltage transmission grid but are mostly unfounded for distribution and microgrids, where the resistance and inductance of the transmission lines are comparable.¹² In addition, losses become more considerable in magnitude when the transmitted power is large. This manuscript puts forth a study of the system in full form, not discarding the interplay of susceptance and conductance, i.e., fully integrating losses, by taking a perturbation theory approach to the losses.

III. EQUILIBRIA AND LINEAR STABILITY ANALYSIS

A. Equilibrium states of power grid operation

The stationary operation of the voltages and power-angles of the machines comprising the power grid is the cornerstone of operability of power grids. Constant voltages and perfect phase-locking, i.e., a point in configuration space where all E_j , ω_j and $\delta_j - \delta_\ell$ are constant in time, is the desired state. The latter restriction requires that all machines rotate at the same frequency, giving the time evolution of the phases $\delta_j(t) = \Omega t + \delta_j^\circ$ for all $j = 1, \dots, N$, leading to the conditions

$$\dot{\omega}_j = \dot{E}_j = 0, \quad \dot{\delta}_j = \Omega, \quad \forall j = 1, \dots, N. \quad (4)$$

In dynamical system terms, this is a stable limit cycle of the system, also known as an isolated closed orbit. From a physical perspective, all points on the limit cycle are equivalent as they only differ by a global phase α , which is irrelevant for the operation of the power grid. One can thus choose one of these points as a representative of the limit cycle and refer to it as an “equilibrium.” The superscript $^\circ$ is used to denote the values of the rotor-phase angle, frequency, and voltage in this equilibrium manifold. Likewise, perturbations along

the limit cycle do not affect the power grid operation and can thus be excluded from the stability analysis.

For the third-order model (3), an equilibrium of the power grid is given by the nonlinear algebraic equations

$$\begin{aligned}\Omega &= \omega_j^\circ, \\ 0 &= P_j^m - D_j \Omega - \sum_{\ell=1}^N E_j^\circ E_\ell^\circ [B_{j,\ell} \sin(\delta_j^\circ - \delta_\ell^\circ) + G_{j,\ell} \cos(\delta_j^\circ - \delta_\ell^\circ)],\end{aligned}\quad (5)$$

$$0 = E_j^f - E_j^\circ + (X_j - X_j') \sum_{\ell=1}^N E_\ell^\circ [B_{j,\ell} \cos(\delta_j^\circ - \delta_\ell^\circ) - G_{j,\ell} \sin(\delta_j^\circ - \delta_\ell^\circ)],$$

noting that many equilibria—stable and unstable—can exist in networks with sufficiently complex topology, although this does not preclude performing a linear stability analysis.^{23,47–50}

B. Linear stability analysis

A central tool of dynamical systems study is linear or small-signal stability analysis.^{51,52} The local stability properties of an equilibrium $(\delta_j^\circ, \omega_j^\circ, E_j^\circ)$, i.e., stability with respect to small perturbations around an equilibrium point, can be obtained by linearizing the equations of motion of the system (3).

To perform a linear stability analysis of (3), one can introduce the perturbations ξ_j , v_j , and ϵ_j , such that

$$\delta_j^{\text{lin}}(t) = \delta_j^\circ + \xi_j(t), \quad \omega_j^{\text{lin}}(t) = \omega_j^\circ + v_j(t), \quad E_j^{\text{lin}}(t) = E_j^\circ + \epsilon_j(t). \quad (6)$$

The rotor angle perturbation ξ_j , the frequency perturbation v_j , and the voltage perturbation ϵ_j can, individually or collectively, decay to zero or grow indefinitely. The fixed point $(\delta_j^\circ, \omega_j^\circ, E_j^\circ)$ is either stable or unstable, correspondingly. This is also known as “exponential stability” or “small-signal stability.” This, on the other hand, does not exclude the existence of other attractors in state space, but the linearization around a fixed point will only preserve the correct dynamical behavior close to the treated fixed point.

Applying the linearization of (3) while simultaneously gauging onto a rotating frame of reference, with rotation frequency Ω as in (4), yields

$$\begin{aligned}\dot{\xi}_j &= v_j, \\ M_j \dot{v}_j &= -D_j v_j - \sum_{\ell=1}^N (\Lambda_{j,\ell} + \Gamma_{j,\ell}) \xi_\ell + \sum_{\ell=1}^N (A_{\ell,j} + C_{j,\ell}) \epsilon_\ell, \\ T_j \dot{\epsilon}_j &= -\epsilon_j + (X_j - X_j') \sum_{\ell=1}^N (H_{j,\ell} + K_{j,\ell}) \epsilon_\ell \\ &\quad + (X_j - X_j') \sum_{\ell=1}^N (A_{j,\ell} + F_{j,\ell}) \xi_\ell,\end{aligned}\quad (7)$$

where matrices $\mathbf{A}, \mathbf{\Gamma}, \mathbf{A}, \mathbf{C}, \mathbf{F}, \mathbf{H}$, and $\mathbf{K} \in \mathbb{R}^{N \times N}$ (written in component form above) are given by

$$\begin{aligned} \Lambda_{j,\ell} &= \begin{cases} -E_j^\circ E_\ell^\circ B_{j,\ell} \cos(\delta_\ell^\circ - \delta_j^\circ) & \text{for } j \neq \ell, \\ \sum_{k \neq j} E_j^\circ E_k^\circ B_{j,k} \cos(\delta_k^\circ - \delta_j^\circ) & \text{for } j = \ell, \end{cases} \\ \Gamma_{j,\ell} &= \begin{cases} -E_j^\circ E_\ell^\circ G_{j,\ell} \sin(\delta_\ell^\circ - \delta_j^\circ) & \text{for } j \neq \ell, \\ \sum_{k \neq j} E_j^\circ E_k^\circ G_{j,k} \sin(\delta_k^\circ - \delta_j^\circ) & \text{for } j = \ell, \end{cases} \\ A_{j,\ell} &= \begin{cases} -E_\ell^\circ B_{j,\ell} \sin(\delta_\ell^\circ - \delta_j^\circ) & \text{for } j \neq \ell, \\ \sum_k E_k^\circ B_{j,k} \sin(\delta_k^\circ - \delta_j^\circ) & \text{for } j = \ell, \end{cases} \\ C_{j,\ell} &= \begin{cases} -E_j^\circ G_{j,\ell} \cos(\delta_\ell^\circ - \delta_j^\circ) & \text{for } j \neq \ell, \\ -E_j^\circ G_{j,\ell} - \sum_k E_k^\circ G_{j,k} \cos(\delta_k^\circ - \delta_j^\circ) & \text{for } j = \ell, \end{cases} \\ F_{j,\ell} &= \begin{cases} E_\ell^\circ G_{j,\ell} \cos(\delta_\ell^\circ - \delta_j^\circ) & \text{for } j \neq \ell, \\ -\sum_{k \neq j} E_k^\circ G_{j,k} \cos(\delta_k^\circ - \delta_j^\circ) & \text{for } j = \ell, \end{cases} \\ H_{j,\ell} &= B_{j,\ell} \cos(\delta_\ell^\circ - \delta_j^\circ), \\ K_{j,\ell} &= G_{j,\ell} \sin(\delta_\ell^\circ - \delta_j^\circ). \end{aligned} \quad (8)$$

The diagonal matrices $\mathbf{M}, \mathbf{D}, \mathbf{X}$, and \mathbf{T} (all in $\mathbb{R}^{N \times N}$) comprise the elements $M_j, D_j, (X_j - X_j^\circ)$, and T_j for $j = 1, \dots, N$, respectively. All these diagonal matrices are positive definite.

The linearized system (7) takes a compact matrix formulation, where the linearized terms are elegantly combined into the Jacobian matrix $\mathbf{J} \in \mathbb{R}^{3N \times 3N}$, by defining the vectors $\boldsymbol{\xi} = (\xi_1, \dots, \xi_N)^\top$, $\mathbf{v} = (v_1, \dots, v_N)^\top$, and $\boldsymbol{\epsilon} = (\epsilon_1, \dots, \epsilon_N)^\top$, each in \mathbb{R}^N , with the superscript \top denoting the transpose of a matrix or vector. The linearized equations can be written as

$$\frac{d}{dt} \begin{pmatrix} \boldsymbol{\xi} \\ \mathbf{v} \\ \boldsymbol{\epsilon} \end{pmatrix} = \mathbf{J} \begin{pmatrix} \boldsymbol{\xi} \\ \mathbf{v} \\ \boldsymbol{\epsilon} \end{pmatrix}, \quad (9)$$

with

$$\mathbf{J} = \begin{pmatrix} \mathbf{0} & \mathbf{1} & \mathbf{0} \\ -\mathbf{M}^{-1}(\mathbf{A} + \mathbf{\Gamma}) & -\mathbf{M}^{-1}\mathbf{D} & \mathbf{M}^{-1}(\mathbf{A}^\top + \mathbf{C}) \\ \mathbf{T}^{-1}\mathbf{X}(\mathbf{A} + \mathbf{F}) & \mathbf{0} & \mathbf{T}^{-1}(\mathbf{X}(\mathbf{H} + \mathbf{K}) - \mathbf{1}) \end{pmatrix}. \quad (10)$$

The Jacobian \mathbf{J} can be brought to a different form that clearly portrays the interplay between the matrices comprising the susceptance $B_{j,\ell}$ and the conductance terms $G_{j,\ell}$ of the power lines and machines,

$$\begin{aligned} \mathbf{J} &= \begin{pmatrix} \mathbf{1} & \mathbf{0} & \mathbf{0} \\ \mathbf{0} & \mathbf{M}^{-1} & \mathbf{0} \\ \mathbf{0} & \mathbf{0} & \mathbf{T}^{-1}\mathbf{X} \end{pmatrix} \\ &\times \left[\begin{pmatrix} \mathbf{0} & \mathbf{1} & \mathbf{0} \\ -\mathbf{A} & -\mathbf{D} & \mathbf{A}^\top \\ \mathbf{A} & \mathbf{0} & \mathbf{H} - \mathbf{X}^{-1} \end{pmatrix} + \begin{pmatrix} \mathbf{0} & \mathbf{0} & \mathbf{0} \\ -\mathbf{\Gamma} & \mathbf{0} & \mathbf{C} \\ \mathbf{F} & \mathbf{0} & \mathbf{K} \end{pmatrix} \right]. \end{aligned} \quad (11)$$

This decomposition is conspicuously designed to work out the impact of Ohmic losses. The left matrix in the square brackets includes all terms that are present in a lossless grid, and the right matrix composed of the block matrices $\mathbf{\Gamma}, \mathbf{C}, \mathbf{F}$, and \mathbf{K} embodies all the matrices associated with resistive losses. The cleavage into two parts will prove useful hence onward.

C. Linear stability and eigenvalues of the Jacobian

An equilibrium $(\delta_j^\circ, \omega_j^\circ, E_j^\circ)$ is linearly stable if perturbations in the linearized system (7) decay exponentially. In general, this is the case if and only if all eigenvalues of the Jacobian matrix \mathbf{J} have a negative real part.^{52,53}

In the present case, one has to take into account that the dynamical system incorporates a fundamental symmetry,

$$\begin{aligned} \Psi_\alpha : \boldsymbol{\delta} &\mapsto \boldsymbol{\delta} + \alpha \mathbf{1}, \\ \mathbb{S}^N &\rightarrow \mathbb{S}^N, \end{aligned} \quad (12)$$

where $\mathbf{1}$ is a vector of ones and $\alpha \in \mathbb{R}$. A shift of all nodal phase angles by a constant value does not have any physical effects: all flows, currents, and stability properties remain unaffected. A geometric interpretation of this symmetry is obtained by viewing the desired operation of the power grid as a limit cycle. As all points along the cycle are equivalent for power grid operation, one can take an arbitrary point as a representative of the limit cycle and refer to it as “the equilibrium.”

As a consequence of this symmetry, any perturbation corresponding to a global phase shift or a shift along the limit cycle, respectively, should be excluded from the stability analysis. This perturbation is encoded in the eigenvector

$$\begin{pmatrix} \boldsymbol{\xi} \\ \mathbf{v} \\ \boldsymbol{\epsilon} \end{pmatrix} = \begin{pmatrix} \mathbf{1} \\ \mathbf{0} \\ \mathbf{0} \end{pmatrix}, \quad (13)$$

with the associated eigenvalue $\mu = 0$. To exclude this mode from the stability analysis, we restrict ourselves to perturbations in orthogonal subspaces defined as

$$\begin{aligned} \mathcal{D}_\perp^{(3)} &= \{(\boldsymbol{\xi}, \mathbf{v}, \boldsymbol{\epsilon}) \in \mathbb{R}^{3N} | (\mathbf{1}, \mathbf{0}, \mathbf{0})^\top (\boldsymbol{\xi}, \mathbf{v}, \boldsymbol{\epsilon}) = 0\}, \\ \mathcal{D}_\perp^{(2)} &= \{(\boldsymbol{\xi}, \boldsymbol{\epsilon}) \in \mathbb{R}^{2N} | (\mathbf{1}, \mathbf{0})^\top (\boldsymbol{\xi}, \boldsymbol{\epsilon}) = 0\}, \\ \mathcal{D}_\perp^{(1)} &= \{\boldsymbol{\xi} \in \mathbb{R}^N | \mathbf{1}^\top \boldsymbol{\xi} = 0\}. \end{aligned} \quad (14)$$

These subspaces are always one dimension smaller than the over-branching space. The subscript $\mathcal{D}_\perp^{(\cdot)}$ refers to the orthogonality devised here, i.e., these spaces are orthogonal to the stable manifold.

Having defined the spaces of operation, one turns to the Jacobian matrix (11) to unravel the definition of linear stability. Consider the eigenvalues $\mu_1, \mu_2, \dots, \mu_{3N} \in \mathbb{C}^{3N}$ of the Jacobian defined via

$$\mathbf{J} \begin{pmatrix} \boldsymbol{\xi} \\ \mathbf{v} \\ \boldsymbol{\epsilon} \end{pmatrix} = \mu \begin{pmatrix} \boldsymbol{\xi} \\ \mathbf{v} \\ \boldsymbol{\epsilon} \end{pmatrix}. \quad (15)$$

There is always one vanishing eigenvalue $\mu_1 = 0$ corresponding to the global shift of all nodal phases, as discussed above. One excludes this mode from the definition of stability and orders the remaining eigenvalues according to their real parts, without loss of generality,

$$\mu_1 = 0, \quad \Re(\mu_2) \leq \Re(\mu_3) \leq \dots \leq \Re(\mu_{3N}). \quad (16)$$

D. Alternative formulations of the eigenvalue problem

We note that the eigenvalue problem (15) can be reformulated in different ways, which are useful for both analytic studies

and numerical computation. First, one can obtain the eigenvalues μ from a generalized eigenvalue problem,

$$\begin{pmatrix} -\Lambda - \Gamma & \mathbf{0} & A^\top + C \\ A + F & \mathbf{0} & H - X^{-1} + K \\ \mathbf{0} & M & \mathbf{0} \end{pmatrix} \begin{pmatrix} \xi \\ v \\ \epsilon \end{pmatrix} = \mu \begin{pmatrix} D & M & \mathbf{0} \\ \mathbf{0} & \mathbf{0} & X^{-1}T \\ M & \mathbf{0} & \mathbf{0} \end{pmatrix} \begin{pmatrix} \xi \\ v \\ \epsilon \end{pmatrix}. \quad (17)$$

To see this, we decompose the original problem (15) in components

$$v = \mu \xi, \quad (18a)$$

$$-M^{-1}((\Lambda + \Gamma)\xi + Dv - (A^\top + C)\epsilon) = \mu v, \quad (18b)$$

$$T^{-1}X((A + F)\xi + (H - X^{-1} + K)\epsilon) = \mu \epsilon. \quad (18c)$$

We multiply (18a) with M and (18c) with $X^{-1}T$. Furthermore, we substitute (18a) in (18b) and multiply the resulting equation with M and obtain

$$\begin{aligned} Mv &= \mu M\xi, \\ -(\Lambda + \Gamma)\xi + (A^\top + C)\epsilon &= \mu(Mv + D\xi), \\ (A + F)\xi + (H - X^{-1} + K)\epsilon &= \mu X^{-1}T\epsilon. \end{aligned} \quad (19)$$

In matrix form, this leads to (17).

Second, one can obtain the eigenvalue μ from a nonlinear eigenvalue problem in a lower dimensional space

$$\left[\begin{pmatrix} -\Lambda - \Gamma & A^\top + C \\ A + F & H - X^{-1} + K \end{pmatrix} - \mu \begin{pmatrix} D & \mathbf{0} \\ \mathbf{0} & X^{-1}T \end{pmatrix} - \mu^2 \begin{pmatrix} M & \mathbf{0} \\ \mathbf{0} & \mathbf{0} \end{pmatrix} \right] \times \begin{pmatrix} \xi \\ \epsilon \end{pmatrix} = \begin{pmatrix} \mathbf{0} \\ \mathbf{0} \end{pmatrix}. \quad (20)$$

The remaining component of the eigenvector is then fixed as $v = \mu \xi$. We derive this reformulation starting again from the decomposition (18). Substituting (18a) into (18b) and multiplying with M eliminates v . Furthermore, we multiply (18c) with $X^{-1}T$ and obtain

$$\begin{aligned} -(\Lambda + \Gamma)\xi + (A^\top + C)\epsilon - \mu D\xi - \mu^2 M\xi &= 0, \\ (A + F)\xi + (H - X^{-1} + K)\epsilon - \mu X^{-1}T\epsilon &= 0. \end{aligned} \quad (21)$$

In matrix form, this results in (20). With this in hand, we now introduce the main lemmata of this work that shall pave the way to several analytical criteria in the later sections.

IV. ANALYTIC STABILITY RESULTS

A. The lossless case

The lossless case was previously analyzed in detail in Ref. 42, so we only review the essential results very briefly. Most importantly, linear stability is determined by a reduced, Hermitian Jacobian matrix. We state this result in the following lemma.

Lemma 1. The linear stability of an equilibrium $(\delta_j^\circ, \omega_j^\circ, E_j^\circ)$ is determined by the reduced Jacobian

$$\Xi = \begin{pmatrix} -\Lambda & A^\top \\ A & H - X^{-1} \end{pmatrix}. \quad (22)$$

The equilibrium is stable if Ξ is negative definite on $\mathcal{D}_\perp^{(2)}$. It is unstable if Ξ is not negative semi-definite.

Proof. Define the Lyapunov function candidate

$$V = \begin{pmatrix} v \\ \xi \\ \epsilon \end{pmatrix}^\top \underbrace{\begin{pmatrix} M & \mathbf{0} & \mathbf{0} \\ \mathbf{0} & \Lambda & -A^\top \\ \mathbf{0} & -A & -(H - X^{-1}) \end{pmatrix}}_{=P} \begin{pmatrix} v \\ \xi \\ \epsilon \end{pmatrix}. \quad (23)$$

Then one can find

$$\begin{aligned} \dot{V} &= -\dot{v}^\top M v - v^\top M \dot{v} + \dot{\xi}^\top \Lambda \xi + \xi^\top \Lambda \dot{\xi} - \dot{\epsilon}^\top A \xi - \epsilon^\top A \dot{\xi} \\ &\quad - \dot{\xi}^\top A^\top \epsilon - \xi^\top A^\top \dot{\epsilon} - \dot{\epsilon}^\top (H - X^{-1}) \epsilon - \epsilon^\top (H - X^{-1}) \dot{\epsilon} \\ &= -2v^\top D v - 2[\xi^\top A^\top X T^{-1} A \dot{\xi} \\ &\quad + \epsilon^\top (H - X^{-1}) X T^{-1} A \dot{\xi} \\ &\quad + \xi^\top A^\top T^{-1} X (H - X^{-1}) \dot{\epsilon} \\ &\quad + \epsilon^\top (H - X^{-1}) T^{-1} X (H - X^{-1}) \dot{\epsilon}] \\ &= -2v^\top D v \\ &\quad - 2[\xi^\top A^\top + \epsilon^\top (H - X^{-1})] X T^{-1} [A \dot{\xi} + (H - X^{-1}) \dot{\epsilon}] \\ &< 0. \end{aligned} \quad (24)$$

The last inequality follows as the matrices X , T , and D are diagonal with only positive entries. If Ξ is negative definite, then P is positive definite and the equilibrium is stable according to Lyapunov's stability theorem. If Ξ is not negative semi-definite, then also P is not positive semi-definite and the equilibrium is unstable according to Lyapunov's instability theorem. \square

The reduced Jacobian can be further decomposed into the subspace corresponding to perturbations of the angles or voltages, respectively. This is especially helpful for the derivation of rigorous stability criteria, cf. Ref. 42.

Lemma 2 (Sufficient and necessary stability conditions for lossless systems).

- I. The equilibrium $(\delta_j^\circ, \omega_j^\circ, E_j^\circ)$ of the lossless grid is linearly stable if (a) the matrix Λ is positive definite on $\mathcal{D}_\perp^{(1)}$ and (b) the matrix $H - X^{-1} + A\Lambda^+A^\top$ is negative definite, where \cdot^+ is the Moore–Penrose pseudoinverse. The equilibrium is unstable if any of the two matrices is not negative semi-definite.
- II. The equilibrium $(\delta_j^\circ, \omega_j^\circ, E_j^\circ)$ of the lossless grid is linearly stable if (a) the matrix $H - X^{-1}$ is negative definite and (b) the matrix $\Lambda + A^\top(H - X^{-1})^{-1}A$ is positive definite on $\mathcal{D}_\perp^{(1)}$. The equilibrium is unstable if any of the two matrices is not negative semi-definite.

This result follows from Lemma 1 by applying the Schur complement, where some care has to be taken to distinguish definiteness

and semi-definiteness as well as about the domain of the matrices.⁵⁴ Details are given in Sharafutdinov *et al.*⁴²

B. The lossy case

We now drop the simplification of a lossless grid and analyze how the presence of resistive terms alters the linear stability of the grid. Complete rigorous results are hard to obtain as the relevant matrices are no longer Hermitian. In particular, the one-to-one correspondence between the definiteness and the signs of the eigenvalues does no longer apply. However, we show that the above results can be generalized in a straightforward way to leading order in the losses.

The starting point of our analysis is the generalized eigenvalue problem (17) which is written in shorthand as

$$\mathcal{A}x_n = \mu_n \mathcal{B}x_n. \quad (25)$$

The matrix \mathcal{A} is decomposed into its Hermitian and anti-Hermitian part,

$$\mathcal{A} = \mathcal{A}_H + \varepsilon \mathcal{A}_A. \quad (26)$$

The anti-Hermitian part \mathcal{A}_A scales with the Ohmic losses and is absent in the lossless case. The key idea of this section is to treat this matrix as a small perturbation. Then, we can show the following results. (i) The unperturbed case can be treated as in the lossless case, leading to a reduced Jacobian. (ii) The perturbations affect the stability equilibrium—encoded in the real part of the eigenvalues—only to quadratic order in the losses. Hence, the impact of Ohmic losses on the linear stability of an equilibrium can be studied to leading order via a reduced Jacobian.

The central objective of interest is again the reduced Jacobian Ξ , which now reads

$$\Xi = \begin{pmatrix} -\Lambda - \Gamma & A^\top + C, \\ A + F & H - X^{-1} + K \end{pmatrix}. \quad (27)$$

For the further analysis, we decompose it into its Hermitian and anti-Hermitian part, $\Xi = \Xi_H + \Xi_A$, with

$$\begin{aligned} \Xi_H &= \frac{1}{2} (\Xi + \Xi^\top) \\ &= \begin{pmatrix} -\Lambda - \Gamma^d & A^\top + N \\ A + N & H - X^{-1} \end{pmatrix}, \\ \Xi_A &= \frac{1}{2} (\Xi - \Xi^\top), \end{aligned} \quad (28)$$

with the Hermitian matrices

$$\begin{aligned} \Gamma^d &= \frac{1}{2} (\Gamma + \Gamma^\top), \\ N &= \frac{1}{2} (C + F). \end{aligned} \quad (29)$$

One can find that these matrices are all *diagonal* with entries

$$\begin{aligned} \Gamma_{jj}^d &= \sum_{k \neq j}^N E_j^\circ E_k^\circ G_{j,k} \sin(\delta_k^\circ - \delta_j^\circ), \\ N_{jj} &= \sum_{k \neq j}^N E_k^\circ G_{j,k} \cos(\delta_k^\circ - \delta_j^\circ). \end{aligned} \quad (30)$$

Lemma 3. *The eigenvalues of the Jacobian are given by the Hermitian generalized eigenvalue problem*

$$\begin{pmatrix} -\Lambda - \Gamma^d & A^\top + N & 0 \\ A + N & H - X^{-1} & 0 \\ 0 & 0 & M \end{pmatrix} x_n = \mu_n \begin{pmatrix} D & 0 & M \\ 0 & X^{-1}T & 0 \\ M & 0 & 0 \end{pmatrix} x_n, \quad (31)$$

up to corrections of quadratic order in Ξ_A , assuming that the eigenvalues are semi-simple.

Proof. The result is proven using a standard perturbation theory argument, treating Ξ_A as a small perturbation. For the sake of convenience, we abbreviate the matrices in the generalized eigenvalue problem (17) such that we have the equation

$$\mathcal{A}x_n = \mu_n \mathcal{B}x_n. \quad (32)$$

We write

$$\mathcal{A} = \mathcal{A}_H + \varepsilon \mathcal{A}_A, \quad (33)$$

where \mathcal{A}_H is the Hermitian part and \mathcal{A}_A is the anti-Hermitian part treated as a perturbation. We note that most examples in the literature are restricted to Hermitian definite problems, i.e., problems where both matrices are Hermitian and \mathcal{B} is also positive definite. This is not the case even for the unperturbed system $\varepsilon = 0$, as \mathcal{B} is not definite such that a very careful analysis is needed.

We now expand eigenstates and eigenvalues as

$$\begin{aligned} \mu_n &= \mu_n^{(0)} + \varepsilon \mu_n^{(1)} + \varepsilon^2 \mu_n^{(2)} + \dots, \\ x_n &= x_n^{(0)} + \varepsilon x_n^{(1)} + \varepsilon^2 x_n^{(2)} + \dots, \end{aligned} \quad (34)$$

and substitute this ansatz into the generalized eigenvalue problem. To zeroth order in ε , we obtain

$$\mathcal{A}_H x_n^{(0)} = \mu_n^{(0)} \mathcal{B} x_n^{(0)}, \quad (35)$$

that is, we obtain (31). The unperturbed eigenvectors can be chosen to be orthogonal with respect to the matrix \mathcal{B} ,

$$x_m^{(0)\top} \mathcal{B} x_n^{(0)} = 0, \quad \text{if } \mu_n^{(0)} \neq \mu_m^{(0)}. \quad (36)$$

This property, well known for ordinary eigenvalue problems, extends to Hermitian generalized eigenvalue problems as one can check by a direct computation,

$$\begin{aligned} \mu_n^{(0)} x_m^{(0)\top} \mathcal{B} x_n^{(0)} &= x_m^{(0)\top} \mathcal{A} x_n^{(0)} = (\mathcal{A}^\top x_m^{(0)})^\top x_n^{(0)} \\ &= \mu_m^{(0)} (\mathcal{B}^\top x_m^{(0)})^\top x_n^{(0)} = \mu_m^{(0)} x_m^{(0)\top} \mathcal{B} x_n^{(0)}, \end{aligned}$$

which is only possible if (36) holds. We now turn back to the perturbed problem. To first order in ε , we obtain

$$\mathcal{A}_A x_n^{(0)} + \mathcal{A}_H x_n^{(1)} = \mu_n^{(0)} \mathcal{B} x_n^{(1)} + \mu_n^{(1)} \mathcal{B} x_n^{(0)}. \quad (37)$$

Multiplying from the left by $\mathbf{x}_n^{(0)\top}$ and exploiting that $\mathbf{x}_n^{(0)\top} \mathcal{A}_H = \mu_n^{(0)} \mathbf{x}_n^{(0)\top} \mathcal{B}$ yields

$$\mu_n^{(1)} = \frac{\mathbf{x}_n^{(0)\top} \mathcal{A}_A \mathbf{x}_n^{(0)}}{\mathbf{x}_n^{(0)\top} \mathcal{B} \mathbf{x}_n^{(0)}}. \quad (38)$$

Now we can use the fact that \mathcal{A}_A is anti-symmetric to obtain

$$\begin{aligned} \mathbf{x}_n^{(0)\top} \mathcal{A}_A \mathbf{x}_n^{(0)} &= (\mathbf{x}_n^{(0)\top} \mathcal{A}_A \mathbf{x}_n^{(0)})^\top \\ &= \mathbf{x}_n^{(0)\top} \mathcal{A}_A^\top \mathbf{x}_n^{(0)} = -\mathbf{x}_n^{(0)\top} \mathcal{A}_A \mathbf{x}_n^{(0)}. \end{aligned} \quad (39)$$

Hence, we have

$$\mathbf{x}_n^{(0)\top} \mathcal{A}_A \mathbf{x}_n^{(0)} = 0 \Rightarrow \mu_n^{(1)} = 0. \quad (40)$$

That is, the linear order correction to the eigenvalues vanishes, leaving terms of quadratic or higher order. \square

We conclude that—to leading order in the losses—only the Hermitian part of the Jacobian is relevant for stability. We can generalize all results from the lossless case if we replace the reduced Jacobian (22) by the matrix Ξ_H defined in (28). In particular, Lemma 2 is generalized as follows.

Lemma 4. *To leading order in the Ohmic losses the linear stability of an equilibrium $(\delta_j^\circ, \omega_j^\circ, E_j^\circ)$ is determined by the Hermitian part of the reduced Jacobian matrix: stable if Ξ_H is negative definite on $\mathcal{D}_\perp^{(2)}$ and unstable if Ξ_H is not negative semi-definite. Stability conditions for this matrix can be decomposed as follows:*

- I. *The matrix Ξ_H is negative definite on $\mathcal{D}_\perp^{(2)}$ if (a) the matrix $\Lambda + \Gamma^d$ is positive definite on $\mathcal{D}_\perp^{(1)}$ and (b) the matrix $\mathbf{H} - \mathbf{X}^{-1} + (\mathbf{A} + \mathbf{N})(\Lambda + \Gamma^d)^+ (\mathbf{A} + \mathbf{N})^\top$ is negative definite. The matrix Ξ_H is non-negative semi-definite if any of the two matrices is not negative semi-definite.*
- II. *The matrix Ξ_H is negative definite on $\mathcal{D}_\perp^{(2)}$ if (a) the matrix $\mathbf{H} - \mathbf{X}^{-1}$ is negative definite and (b) the matrix $(\Lambda + \Gamma^d) + (\mathbf{A} + \mathbf{N})^\top (\mathbf{H} - \mathbf{X}^{-1})^{-1} (\mathbf{A} + \mathbf{N})$ is positive definite on $\mathcal{D}_\perp^{(1)}$. The matrix Ξ_H is non-negative semi-definite if any of the two matrices is not negative semi-definite.*

We will henceforth work with Lemma 4, where we note that the lossless case is recovered when $\Gamma^d = \mathbf{N} = \mathbf{0}$ and we return to Lemma 2.

C. Sufficient stability conditions for the lossy case

Our previous reasoning shows that the stability in a lossy grid is described by the Hermitian matrix Ξ_H —up to corrections of quadratic order in the Ohmic losses. While this approach is very convenient and enables further analytic studies, it does not give any quantitative results on the magnitude of the corrections. Here, we provide a rigorous sufficient stability condition that generalizes the condition of negative definiteness of the reduced Jacobian in Lemma 1.

Lemma 5. *Let $(\delta_j^\circ, \omega_j^\circ, E_j^\circ)$ be an equilibrium of the lossy grid. The equilibrium is stable if for all vectors $\mathbf{x} \in \{\mathbb{C}^{2N} | \mathbf{x} \neq \mathbf{0}, (\mathbf{1}^\top, \mathbf{0}^\top) \mathbf{x} = 0\}$*

$\neq \mathbf{0}, (\mathbf{1}^\top, \mathbf{0}^\top) \mathbf{x} = 0\}$

$$\mathbf{x}^\dagger \Xi_H \mathbf{x} < \frac{(\mathbf{x}^\dagger \Psi \mathbf{x})}{(\mathbf{x}^\dagger \Phi \mathbf{x})^2} (\mathbf{x}^\dagger \Xi_A \mathbf{x})^2 \quad (41)$$

with the abbreviations

$$\Phi = \begin{pmatrix} D & \mathbf{0} \\ \mathbf{0} & T\mathbf{X}^{-1} \end{pmatrix}, \quad \Psi = \begin{pmatrix} M & \mathbf{0} \\ \mathbf{0} & \mathbf{0} \end{pmatrix}. \quad (42)$$

Proof. We start from the nonlinear eigenvalue problem (20) and multiply from the left with the Hermitian conjugate of the eigenstate $(\xi^\dagger, \epsilon^\dagger)$ to obtain the algebraic equation

$$\eta_1 + \eta_2 \mu + \eta_3 \mu^2 = 0, \quad (43)$$

with

$$\begin{aligned} \eta_1 &= -\left(\begin{pmatrix} \xi \\ \epsilon \end{pmatrix}^\dagger \Xi \begin{pmatrix} \xi \\ \epsilon \end{pmatrix}\right), \\ \eta_2 &= \left(\begin{pmatrix} \xi \\ \epsilon \end{pmatrix}^\dagger \Phi \begin{pmatrix} \xi \\ \epsilon \end{pmatrix}\right) > 0, \\ \eta_3 &= \left(\begin{pmatrix} \xi \\ \epsilon \end{pmatrix}^\dagger \Psi \begin{pmatrix} \xi \\ \epsilon \end{pmatrix}\right) \geq 0. \end{aligned} \quad (44)$$

The coefficients η_2 and η_3 are real and non-negative as the matrices D, M, T , and X are diagonal with strictly positive entries (except for the trivial case $\xi = \mathbf{0}$ for which $\eta_3 = 0$). We first consider the case $\eta_3 = 0$ for which $\mu = -\eta_1/\eta_2$. Hence, we immediately see that if Ξ_H is negative definite, we have $\Re(\mu) < 0$.

Now assume $\eta_3 > 0$. For the remaining coefficient η_1 , we write

$$\begin{aligned} \eta_1 &= \alpha + i\beta, \\ \Rightarrow \alpha &= -\left(\begin{pmatrix} \xi \\ \epsilon \end{pmatrix}^\dagger \Xi_H \begin{pmatrix} \xi \\ \epsilon \end{pmatrix}\right), \\ i\beta &= -\left(\begin{pmatrix} \xi \\ \epsilon \end{pmatrix}^\dagger \Xi_A \begin{pmatrix} \xi \\ \epsilon \end{pmatrix}\right). \end{aligned} \quad (45)$$

The algebraic (43) can now be solved for μ such that

$$\mu = \frac{-\eta_2 \pm \sqrt{\eta_2^2 - 4\eta_3(\alpha + i\beta)}}{2\eta_3}. \quad (46)$$

To ensure stability, the real part of μ needs to be strictly smaller than zero, which translates to

$$\Re\left(\sqrt{\eta_2^2 - 4\eta_3(\alpha + i\beta)}\right) < \eta_2. \quad (47)$$

One can now show by an explicit calculation that this is the case if

$$\alpha > \frac{\eta_3 \beta^2}{\eta_2^2}. \quad (48)$$

Hence, if the assumption (41) is satisfied for all vectors, we indeed have $\Re(\mu) < 0$ and the equilibrium is stable. \square

We note that the lemma can also be stated in a slightly different form, avoiding the complicated assumptions about the domain of the vector \vec{x} . Assuming that the trivial eigenvalue $\mu_1 = 0$ is the only eigenvalue on the imaginary axis, the stability condition (41)

can be relaxed and simplified: we can replace the $<$ sign by \leq in the condition and simplify the domain to $\tilde{x} \neq 0$.

Lemma 5 provides a rigorous sufficient condition for linear stability in lossy grids. However, it might be hard to apply in practice due to its nonlinearity. We now derive a simpler, yet coarser condition by bounding the right-hand side (RHS) in (41). To quantify the overall strength of the Ohmic losses, we consider the following characteristic that is inspired by the degree of a node in a weighted network:

$$\hat{G}_j = |G_{jj}| + \sum_{\ell \neq j} |G_{j\ell}|, \quad (49)$$

as well as the maximum “degree” in the network,

$$\hat{G}_{\max} = \max_j \hat{G}_j. \quad (50)$$

Furthermore, we define $M_{\max} = \max_j M_j$ and

$$\zeta_1 = \max_{j=1,\dots,N} \left(E_j^\circ / \sqrt{D_j} + \sqrt{X_j/T_j} \right), \quad (51)$$

$$\zeta_2 = \max_{j=1,\dots,N} \left[\max \left(E_j^\circ / \sqrt{D_j}, \sqrt{X_j/T_j} \right) \right]. \quad (52)$$

Lemma 6. Let $(\delta_j^\circ, \omega_j^\circ, E_j^\circ)$ be an equilibrium of the lossy grid. If the matrix

$$\Xi_H + M_{\max} \zeta_1^2 \zeta_2^2 \hat{G}_{\max}^2 \mathbb{I} \quad (53)$$

is negative definite on $\mathcal{D}_\perp^{(2)}$, then the equilibrium is stable.

Proof. To prove this statement, we have to bind the right-hand side in (41). Defining $\mathbf{y} = \Phi^{1/2} \mathbf{x}$ and $\mathbf{S} = i \Phi^{-1/2} \Xi_A \Phi^{-1/2}$, we have

$$\frac{(\mathbf{x}^\dagger i \Xi_A \mathbf{x})^2}{(\mathbf{x}^\dagger \Phi \mathbf{x})^2} = \frac{(\mathbf{y}^\dagger \mathbf{S} \mathbf{y})^2}{\|\mathbf{y}\|^4} \leq \rho(\mathbf{S})^2, \quad (54)$$

where $\rho(\mathbf{S})$ is the dominant eigenvalue of the Hermitian matrix \mathbf{S} . We now bound this eigenvalue using Geršgorin’s circle theorem. The diagonal of \mathbf{S} vanishes and so do the centers of the Geršgorin disks. Hence, we find that every eigenvalue γ of \mathbf{S} satisfies $|\gamma| \leq \sum_\ell |S_{j\ell}|$ for some index j such that

$$\rho(\mathbf{S}) \leq \max_{j=1,\dots,2N} \sum_{\ell \neq j} |S_{j\ell}|. \quad (55)$$

Inserting the definition of \mathbf{S} , we have for $j \leq N$

$$\begin{aligned} \sum_\ell |S_{j\ell}| &= \sum_{\ell \neq j} \frac{|\Gamma_{j\ell}|}{\sqrt{D_j D_\ell}} + \frac{1}{2} \sum_\ell \sqrt{\frac{X_\ell}{D_j T_\ell}} |C_{j\ell} - F_{\ell j}| \\ &\leq \sum_{\ell \neq j} \frac{E_j^\circ E_\ell^\circ |G_{j\ell}|}{\sqrt{D_j D_\ell}} + \sum_\ell \sqrt{\frac{X_\ell}{D_j T_\ell}} E_j^\circ |G_{j\ell}| \\ &\leq \frac{E_j^\circ}{\sqrt{D_j}} \zeta_1 \hat{G}_j. \end{aligned}$$

For $j > N$, with $i = j - N$, we obtain

$$\begin{aligned} \sum_\ell |S_{j\ell}| &= \sum_{\ell \neq i} \sqrt{\frac{X_i X_\ell}{T_i T_\ell}} |K_{i\ell}| + \frac{1}{2} \sum_\ell \sqrt{\frac{X_i}{D_\ell T_i}} |F_{i\ell} - C_{\ell,i}| \\ &\leq \sum_{\ell \neq i} \sqrt{\frac{X_i X_\ell}{T_i T_\ell}} |G_{i\ell}| + \sum_\ell \sqrt{\frac{X_i}{D_\ell T_i}} E_\ell^\circ |G_{i\ell}| \\ &\leq \sqrt{\frac{X_i}{T_i}} \zeta_1 \hat{G}_i. \end{aligned}$$

Thus, we find that

$$\rho(\mathbf{S}) \leq \zeta_1 \zeta_2 \hat{G}_{\max}. \quad (56)$$

Furthermore, it is easy to see that

$$(\mathbf{x}^\dagger \Psi \mathbf{x}) \leq M_{\max} \|\mathbf{x}\|^2. \quad (57)$$

Now we use these bounds to prove stability. The negative definiteness of $\Xi_H + M_{\max} \zeta_1^2 \zeta_2^2 \hat{G}_{\max}^2 \mathbb{I}$ implies that for all vectors $\mathbf{x} \in \mathcal{D}_\perp^{(2)}$, we have

$$(\mathbf{x}^\dagger \Xi_H \mathbf{x}) + M_{\max} \zeta_1^2 \zeta_2^2 \hat{G}_{\max}^2 (\mathbf{x}^\dagger \mathbf{x}) < 0. \quad (58)$$

Using the bounds in (56) and (57), we then find

$$\begin{aligned} (\mathbf{x}^\dagger \Xi_H \mathbf{x}) &< -M_{\max} \|\mathbf{x}\|^2 \zeta_1^2 \zeta_2^2 \hat{G}_{\max}^2 \\ &\leq -(\mathbf{x}^\dagger \Psi \mathbf{x}) \frac{(\mathbf{x}^\dagger i \Xi_A \mathbf{x})^2}{(\mathbf{x}^\dagger \Phi \mathbf{x})^2}. \end{aligned} \quad (59)$$

Hence, the condition in Lemma 5 is satisfied and the equilibrium is stable. \square

Analogous to Lemma 5, this lemma can be formulated without the restriction to $\mathcal{D}_\perp^{(2)}$ and with the assumption that there is no eigenvalue, other than the trivial eigenvalue $\mu_1 = 0$, on the imaginary axis.

V. EXPLICIT STABILITY CRITERIA

A. Stability of the rotor angle and voltage systems

The decomposition of the reduced Jacobian in Lemma 4 is of fundamental importance to this work, as it evinces the roles of the rotor angle and the voltage dynamics for the stability of the third-order model.

Consider first the isolated power-angle dynamics, assuming that the voltages E_j remain fixed. Fixing $\epsilon = 0$, the linearized equations of motions read

$$\frac{d}{dt} \begin{pmatrix} \xi \\ \mathbf{v} \end{pmatrix} = \begin{pmatrix} \mathbf{0} & \mathbb{I} \\ -\mathbf{M}^{-1}(\mathbf{A} + \mathbf{\Gamma}) & -\mathbf{M}^{-1}\mathbf{D} \end{pmatrix} \begin{pmatrix} \xi \\ \mathbf{v} \end{pmatrix}. \quad (60)$$

Performing the same simplification as in Sec. IV, one can find that the isolated rotor angle dynamics is linearly stable—to leading order in the losses—if and only if the matrix $\mathbf{A} + \mathbf{\Gamma}^d$ is positive definite on $\mathcal{D}_\perp^{(1)}$.

Similarly, consider the isolated voltage dynamics by assuming that the rotor angle remains fixed. Fixing $\mathbf{v} = \xi = 0$, the linearized

equations of motion read

$$\frac{d}{dt}\epsilon = T^{-1}X(H - X^{-1} + K)\epsilon. \quad (61)$$

Hence, one finds that the isolated voltage dynamics is linearly stable—to leading order in the losses—if and only if the matrix $H - X^{-1}$ is negative definite.

In conclusion, one finds that the criteria I (a) and II (a) in Lemma 4 ensure the stability, to linear order in the losses, of the isolated rotor angle or voltage subsystem, respectively. Linear stability of the entire system is ensured if and only if, in addition, the complementary criteria I (b) or II (b) are satisfied.

To further elucidate the nature of the stability conditions, consider the full stability criterion I in Lemma 4. Assume that criterion I (a) is satisfied, i.e., $\Lambda + \Gamma^d$ is positive definite on $\mathcal{D}_\perp^{(1)}$, and the rotor angle subsystem is linearly stable to leading order in the losses. The complementary criterion I (b), i.e., $H - X^{-1} + (A + N)(\Lambda + \Gamma^d)^+(A + N)^T$, is negative definite. This condition is far stricter than the condition of pure stability of the voltage system, i.e., $H - X^{-1}$ is negative definite. Hence, stability of the two isolated subsystems is not sufficient, instead they must comprise a certain “security margin” in order to maintain linear stability.

Making use of the angle-voltage decomposition, one can derive explicit necessary and sufficient stability criteria. To this end, we first consider the isolated subsystems and subsequently the composite dynamics of the full system. Note that the lossless case has been discussed in Ref. 42; thus, here the focus is placed on the impact of Ohmic losses in leading order.

B. Stability of the voltage system

Criterion II (a) in Lemma 4 entails the stability of the isolated voltage subsystem—up to leading order in the losses. A violation implies the instability of the voltage dynamics, and as a consequence also the instability of the entire system, including the rotor angle and frequency dynamics.

Most remarkably, criterion II (a) includes only the matrices H and X , which are also present in the lossless case.⁴² To leading order, Ohmic losses in the transmission lines thus affect the stability of the voltage system only indirectly via the position of the respective equilibrium, in particular, via the equilibrium rotor angles δ_j° , which enter the matrix H . Due to the similarity to the lossless case, this work refrains from a detailed analysis of the stability of the voltage system and only quotes two results from Sharafutdinov *et al.*⁴²

Corollary 1. *If for all nodes $j = 1, \dots, N$,*

$$(X_j - X'_j)^{-1} > \sum_{\ell=1}^N B_{j,\ell}, \quad (62)$$

then the matrix $H - X^{-1}$ is negative definite.

Corollary 2. *If for any subset of nodes $\mathcal{S} \subset \{1, 2, \dots, N\}$,*

$$\sum_{j \in \mathcal{S}} (X_j - X'_j)^{-1} \leq \sum_{j, \ell \in \mathcal{S}} B_{j,\ell} \cos(\delta_\ell^\circ - \delta_j^\circ), \quad (63)$$

then the matrix $H - X^{-1}$ is not negative definite and the necessary stability condition in Lemma 4 is violated.

C. Rotor angle stability

Criterion I (a) in Lemma 4 entails the stability of the isolated rotor angle subsystem. Briefly take the lossless case into consideration, for which rotor angle stability is determined by the matrix Λ . The isolated subsystem is stable if Λ is positive definite on $\mathcal{D}_\perp^{(1)}$ or, equivalently, if the eigenvalues satisfy $0 < \lambda_2 < \dots < \lambda_N$. One can directly derive sufficient stability criteria in terms of the angle differences in the grid: If for all connections (j, ℓ) in a power grid one has

$$\cos(\delta_j^\circ - \delta_\ell^\circ) > 0, \quad (64)$$

then the isolated rotor angle subsystem is stable. This follows from the fact that Λ is a proper Laplacian matrix of a weighted undirected graph, which is well known to be positive definite on $\mathcal{D}_\perp^{(1)}$. If the condition is not satisfied for a line, the matrix Λ rather describes a signed graph, for which positive definiteness is more involved.⁵⁵ Sufficient and necessary criteria have been obtained in Refs. 56–59.

One can generalize the above condition to power grids with Ohmic losses in the following way.

Corollary 3. *If for all connections (j, ℓ) in a power grid, one has*

$$B_{j,\ell} \cos(\delta_\ell^\circ - \delta_j^\circ) + G_{j,\ell} \sin(\delta_\ell^\circ - \delta_j^\circ) > 0, \quad (65)$$

then the eigenvalue $\lambda_2, \dots, \lambda_N$ of $\Lambda + \Gamma$ has a positive real part and the matrix $\Lambda + \Gamma^d$ is positive definite on $\mathcal{D}_\perp^{(1)}$, such that the isolated angle subsystem is linearly stable to leading order in the losses.

Proof. The statement can be proved by applying Geršgorin's circle theorem⁶⁰ to $\Lambda + \Gamma$. Each eigenvalue of this matrix λ_j is bound to exist in a disk of radius $R_j = \sum_{\ell \neq j} |\Lambda_{j,\ell} + \Gamma_{j,\ell}|$ around the center $\Lambda_{jj} + \Gamma_{jj}$ such that

$$|\lambda_j - (\Lambda_{jj} + \Gamma_{jj})| \leq \sum_{\ell \neq j} |\Lambda_{j,\ell} + \Gamma_{j,\ell}|. \quad (66)$$

If condition (65) is satisfied, one can simplify this relation to

$$|\lambda_j - (\Lambda_{jj} + \Gamma_{jj})| \leq \sum_{\ell \neq j} \Lambda_{j,\ell} + \Gamma_{j,\ell} = (\Lambda_{jj} + \Gamma_{jj}), \quad (67)$$

which directly yields

$$\Re(\lambda_j) \geq 0. \quad (68)$$

Now one further shows that $\lambda_1 = 0$ is the only vanishing eigenvalue of $\Lambda + \Gamma$ such that

$$\Re(\lambda_j) > 0, \quad j = 2, \dots, N. \quad (69)$$

For every non-zero vector $x \in \mathcal{D}_\perp^{(1)}$, we thus have

$$x^T (\Lambda + \Gamma^d) x = \Re[x^T (\Lambda + \Gamma) x] > 0, \quad (70)$$

and $(\Lambda + \Gamma^d)$ is positive definite on $\mathcal{D}_\perp^{(1)}$. \square

We see that even the case of rotor angle stability becomes much more involved in the lossy case due to the presence of the matrix Γ . This holds especially for the interpretation of results in terms of the network structure. In the lossless case, the stability condition can be rephrased as $\lambda_2 > 0$, which is particularly convenient as λ_2 is a measure of the network's algebraic connectivity. Hence,

the stability condition can be interpreted in terms of graph topology and connectivity.⁶¹ This relation no longer applies in the lossy case. In particular, $\mathbf{A} + \mathbf{\Gamma}$ is a Laplacian, but of a directed signed graph. Hence, the eigenvalues are not guaranteed to be real. In contrast, the matrix $\mathbf{A} + \mathbf{\Gamma}^d$ is Hermitian and thus has real eigenvalues, but it is no longer a Laplacian matrix such that the interpretation of its lowest non-zero eigenvalue as a connectivity does no longer hold. However, the relation still holds approximately if we restrict ourselves to the leading order impact of Ohmic losses.

Lemma 7. *To leading order in the losses, the eigenvalues of $\mathbf{A} + \mathbf{\Gamma}$ and $\mathbf{A} + \mathbf{\Gamma}^d$ coincide.*

Proof. In identical fashion to the proof of Lemma 3, consider

$$(\mathbf{A} + \mathbf{\Gamma}) \mathbf{x}_n = \lambda_n \mathbf{x}_n, \quad (71)$$

with \mathbf{x}_n and λ_n being the respective eigenstates and eigenvalues. Separate $\mathbf{A} + \mathbf{\Gamma}$ into Hermitian and anti-Hermitian parts and take the anti-Hermitian part as a perturbation. Consider an expansion of the eigenstates and normalized eigenvalues as in (34). To leading order in the losses,

$$\mathbf{x}_n^{(0)\top} (\mathbf{A} + \mathbf{\Gamma}) \mathbf{x}_n^{(0)} = \mathbf{x}_n^{(0)\top} (\mathbf{A} + \mathbf{\Gamma}^d) \mathbf{x}_n^{(0)} = \lambda_n, \quad (72)$$

thus the eigenvalues of $\mathbf{A} + \mathbf{\Gamma}$ and $\mathbf{A} + \mathbf{\Gamma}^d$ coincide. \square

In the following, we will formulate several stability criteria for the full system applying to the leading order in the losses. We frequently use the eigenvalues λ_2 , which is assumed to be real and interpreted as a connectivity, and the associated eigenvector \mathbf{v}_F called the Fiedler vector.^{61–64} We stress that this is not necessarily true but is appropriate to leading order in the losses as shown above.

D. Mixed instabilities

We now turn to the interplay of voltage and angle stability, i.e., further investigating criteria I (b) and II (b) in Lemma 4. Unless stated otherwise, consider an equilibrium such that the criteria I (a) and II (a) in Lemma 4 are satisfied. Hence, the isolated subsystems are stable, but the full system can still become unstable.

To begin, consider the case where the voltage dynamics are very stiff, i.e., the case where $(X_j - X'_j)$ are small. Recall that in the limit $(X_j - X'_j) \rightarrow 0$, the voltage dynamics are trivially stable such that stability is determined solely by the angular subsystem. One can extend this analysis to the case of small but non-zero $(X_j - X'_j)$ and relate stability to the connectivity of the power grid. The stability of the isolated rotor angle subsystem is ensured if [cf. criterion I (a) in Lemma 4, or Refs. 30 and 42],

$$\Re(\lambda_2) > 0, \quad (73)$$

where λ_2 is the lowest non-zero eigenvalue of the Laplacian $\mathbf{A} + \mathbf{\Gamma}$, interpreted as the algebraic connectivity, which is real to leading order in the Ohmic losses.

Corollary 4. *To leading order in the Ohmic losses, a necessary condition for the stability of an equilibrium point is given by*

$$\lambda_2 > \mathbf{v}_F^\top [\mathbf{A}^\top \mathbf{X} \mathbf{A} + 2\mathbf{A}^\top \mathbf{X} \mathbf{N} + \mathbf{N} \mathbf{X} \mathbf{N}] \mathbf{v}_F + \mathcal{O}((X_j - X'_j)^2), \quad (74)$$

where \mathbf{v}_F denotes the Fiedler vector of the Laplacian $\mathbf{A} + \mathbf{\Gamma}$ for $(X_j - X'_j) \equiv 0$.

Proof. The normalized Fiedler vector, at $(X_j - X'_j) \equiv 0$, is denoted \mathbf{v}_F . The actual normalized Fiedler vector, for a particular non-zero value of the $(X_j - X'_j)$, is denoted \mathbf{v}'_F , such that

$$\mathbf{v}'_F = \mathbf{v}_F + \mathcal{O}((X_j - X'_j)^1). \quad (75)$$

Take the expansion

$$-(\mathbf{H} - \mathbf{X}^{-1})^{-1} = (\mathbf{X}^{-1} - \mathbf{H})^{-1} = \sum_{\ell=0}^{\infty} \mathbf{X}(\mathbf{X}\mathbf{H})^\ell, \quad (76)$$

such that at lowest order one obtains

$$(\mathbf{X}^{-1} - \mathbf{H})^{-1} = \mathbf{X} + \mathcal{O}((X_j - X'_j)^2). \quad (77)$$

Now, criterion II (b) in Lemma 4 can be reformulated as follows: For all non-zero vectors $\mathbf{y} \in \mathbb{C}^N$, we must have

$$\mathbf{y}^\dagger (\mathbf{A} + \mathbf{\Gamma}^d) \mathbf{y} > \mathbf{y}^\dagger (\mathbf{A} + \mathbf{N})^\top (\mathbf{X}^{-1} - \mathbf{H})^{-1} (\mathbf{A} + \mathbf{N}) \mathbf{y}. \quad (78)$$

For a particular choice of \mathbf{y} , one obtains a necessary condition for stability. Taking $\mathbf{y} = \mathbf{v}'_F$, the above results in

$$\lambda_2 > \mathbf{v}_F^\dagger (\mathbf{A} + \mathbf{N})^\top (\mathbf{X}^{-1} - \mathbf{H})^{-1} (\mathbf{A} + \mathbf{N}) \mathbf{v}'_F, \quad (79)$$

where applying the aforementioned expansion on the right-hand side, at leading order in $(X_j - X'_j)$, yields

$$\lambda_2 > \mathbf{v}_F^\dagger (\mathbf{A} + \mathbf{N})^\top \mathbf{X} (\mathbf{A} + \mathbf{N}) \mathbf{v}_F + \mathcal{O}((X_j - X'_j)^2), \quad (80)$$

taking into account that the eigenvalues of $\mathbf{A} + \mathbf{\Gamma}$ and $\mathbf{A} + \mathbf{\Gamma}^d$ coincide to leading order in the lossy case (cf. Lemma 7). Given now the symmetries of \mathbf{A} , \mathbf{N} , and \mathbf{X} , one can expand the result as

$$\lambda_2 > \mathbf{v}_F^\dagger [\mathbf{A}^\top \mathbf{X} \mathbf{A} + 2\mathbf{A}^\top \mathbf{X} \mathbf{N} + \mathbf{N} \mathbf{X} \mathbf{N}] \mathbf{v}_F + \mathcal{O}((X_j - X'_j)^2). \quad (81)$$

This concludes the proof. This corollary entails a previous result in Ref. 42. \square

Note that each term of the matrices on the right-hand side of (74) is symmetric and hence contributes positively, adding to the lower bound on the algebraic connectivity λ_2 of the system. This implies that resistive networks *always* require a higher degree of connectivity to ensure stability.

Corollary 5. *A resistive power grid needs to ensure*

$$\lambda_2 > \sum_j (X_j - X'_j) \mathbf{v}_{Fj}^\top \left(\sum_{k \neq j}^N E_k^\circ G_{j,k} \right), \quad (82)$$

in the limiting case of no power exchange, to leading order in the losses.

Proof. If there is a negligible power exchange in the power grid, all rotor angles $\delta_j^\circ, \forall j$ are identical, such that

$$\cos(\delta_\ell^\circ - \delta_j^\circ) = 1, \quad \sin(\delta_\ell^\circ - \delta_j^\circ) = 0, \quad (83)$$

for all connections (j, ℓ) . This results in $A_{j,\ell} = 0$ and $\Gamma_{jj}^d = 0$ in (8), and Corollary 4 reads

$$\lambda_2 > \mathbf{v}_F^\top \mathbf{N} \mathbf{X} \mathbf{N} \mathbf{v}_F, \quad (84)$$

where all matrices are diagonal matrices. Writing the terms explicitly yields (82), entailing a lower bound to the connectivity of a power

grid with resistive elements while considering only leading order of the losses. \square

Before proceeding with the final corollaries, note that despite the cumbersome matrix notation employed here, one can still extract very useful information—which can easily be computed numerically if desired—by utilizing different *matrix norms*.

Lemma 8. Let $\mathbf{Z} \in \mathbb{C}^{N \times N}$ and $\mathbf{W} \in \mathbb{C}^{N \times N}$ be two matrices, and let $\|\cdot\|_n$ denote an n -induced matrix norm, one has

$$\|\mathbf{ZW}\|_n \leq \|\mathbf{Z}\|_n \|\mathbf{W}\|_n, \quad (85)$$

i.e., all induced matrix norms are sub-multiplicative.

Furthermore, recall that $\|\cdot\|_2$ denotes the ℓ_2 -norm for vectors, also known as *spectral norm* or *Euclidean norm*.

Corollary 6. If a positive algebraic connectivity $\lambda_2 > 0$, and all nodes $j = 1, \dots, N$,

$$(X_j - X_j')^{-1} - \sum_{\ell=1}^N B_{j,\ell} > \frac{\|(\mathbf{A} + \mathbf{N})\|_2 \|(\mathbf{A} + \mathbf{N})^\top\|_2}{\lambda_2}, \quad (86)$$

where $\|\cdot\|_2$ is the induced ℓ_2 -norm, then an equilibrium point is linearly stable to leading order in the losses.

Proof. A positive algebraic connectivity $\lambda_2 > 0$ implies that $\mathbf{A} + \mathbf{\Gamma}^d$ is positive definite on $\mathcal{D}_\perp^{(1)}$, and criterion I (a) in Lemma 4 is satisfied.

Consider now criterion I (b) in Lemma 4. Using Geršgorin's circle theorem, as in the proof of Corollary 3, one finds that condition (86) implies that

$$(\mathbf{X}^{-1} - \mathbf{H}) - \lambda_2^{-1} \|(\mathbf{A} + \mathbf{N})\|_2 \|(\mathbf{A} + \mathbf{N})^\top\|_2 \mathbf{I} \quad (87)$$

is positive definite. Noting that to leading order in the losses, we have $\lambda_2^{-1} = \|(\mathbf{A} + \mathbf{\Gamma})^+\|_2 = \|(\mathbf{A} + \mathbf{\Gamma}^d)^+\|_2$; this implies that $\forall \mathbf{y} \in \mathbb{R}$,

$$\begin{aligned} \mathbf{y}^\top (\mathbf{X}^{-1} - \mathbf{H}) \mathbf{y} &> \|\mathbf{A} + \mathbf{N}\|_2 \|(\mathbf{A} + \mathbf{\Gamma}^d)^+\|_2 \|(\mathbf{A} + \mathbf{N})^\top\|_2 \|\mathbf{y}\|^2 \\ &\geq \|(\mathbf{A} + \mathbf{N})(\mathbf{A} + \mathbf{\Gamma}^d)^+(\mathbf{A} + \mathbf{N})^\top\|_2 \|\mathbf{y}\|^2 \\ &\geq \mathbf{y}^\top (\mathbf{A} + \mathbf{N})(\mathbf{A} + \mathbf{\Gamma}^d)^+(\mathbf{A} + \mathbf{N})^\top \mathbf{y}. \end{aligned} \quad (88)$$

Hence, matrix $\mathbf{H} - \mathbf{X}^{-1} + (\mathbf{A} + \mathbf{N})(\mathbf{A} + \mathbf{\Gamma}^d)^+(\mathbf{A} + \mathbf{N})^\top$ is negative definite and criterion I (b) in Lemma 4 is satisfied. The equilibrium is linearly stable to leading order in the losses. \square

Corollary 7. If by criterion II. (a) in Lemma 4 the matrix $\mathbf{H} - \mathbf{X}^{-1}$ is negative definite, and if the algebraic connectivity λ_2 satisfies

$$\lambda_2 > \|(\mathbf{A} + \mathbf{N})^\top (\mathbf{H} - \mathbf{X}^{-1})^{-1} (\mathbf{A} + \mathbf{N})\|_2, \quad (89)$$

where $\|\cdot\|_2$ is the induced ℓ_2 -norm, then, to leading order in the losses, the equilibrium point is linearly stable.

Proof. Assume that $\mathbf{H} - \mathbf{X}^{-1}$ is negative definite as given by criterion II (a) in Lemma 4. The assumption (89) implies that $\forall \mathbf{y} \in \mathcal{D}_\perp^{(1)}$,

$$\begin{aligned} \mathbf{y}^\top (\mathbf{A} + \mathbf{\Gamma}^d) \mathbf{y} &\geq \lambda_2 \|\mathbf{y}\|^2 \\ &> \|(\mathbf{A} + \mathbf{N})^\top (\mathbf{H} - \mathbf{X}^{-1})^{-1} (\mathbf{A} + \mathbf{N})\|_2 \|\mathbf{y}\|^2 \\ &\geq \mathbf{y}^\top (\mathbf{A} + \mathbf{N})^\top (\mathbf{H} - \mathbf{X}^{-1})^{-1} (\mathbf{A} + \mathbf{N}) \mathbf{y}, \end{aligned} \quad (90)$$

again noticing that the eigenvalues for $(\mathbf{A} + \mathbf{\Gamma}^d)$ and $(\mathbf{A} + \mathbf{\Gamma})$ coincide to leading order. Thus, the matrix $(\mathbf{A} + \mathbf{\Gamma}^d) + (\mathbf{A} + \mathbf{N})^\top (\mathbf{H} - \mathbf{X}^{-1})^{-1} (\mathbf{A} + \mathbf{N})$ is negative definite in $\mathcal{D}_\perp^{(1)}$. Criterion II (b) in Lemma 4 is, therefore, satisfied and the equilibrium is linearly stable to leading order in the losses. \square

VI. NUMERICAL ANALYSIS

In this section, we present a numerical analysis of two model systems to test how tight the bounds given by the above criteria, i.e., Corollaries 1–7 are and ultimately showcase their utility.

First, we consider a system consisting of two machines with one acting as a generator, producing power ($P^m > 0$), and the other acting as a motor, consuming power ($P^m < 0$).^{36,65,66} Second, we consider a system comprised of three motors and three generators, connected in a ring. The topology and parameters are given in Fig. 1. While the active power of each node and the admittance of the lines connecting each node can differ for different nodes, all other parameters, e.g., difference in reactance, damping, inertia, relaxation time, and internal voltages, are set to the same value for each machine. To check the stability boundary, we vary P^m at all nodes proportionally. More precisely, we use the base values in Fig. 1 and set $P_1^m = -P_2^m$, in the case of the two-machine system, or multiply by P_f , in the case of the six-machine system, to change both the output of generator

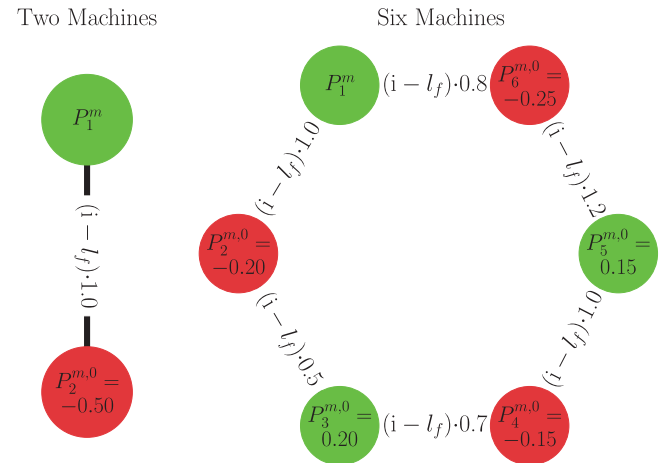


FIG. 1. Topology of the two-machine system and six-machine system that were used in the numerical study. Synchronous generators and motors are indicated by green and red color, respectively. The vertex labels show the default active power at each machine $P_i^{m,0}$. When changing the power input/output of each machine, we will refer to absolute values in the two-machine system, while multiplying each active power by the factor P_f , i.e., $P_i^m = P_f \cdot P_i^{m,0}$, in the six-machine system. The active power P_1^m at the slack is chosen to balance the overall power. The edge labels show the admittance of the lines between the machines with the real part $G_{j,\ell}$ that is associated with losses given by the product of the imaginary part of the admittance $B_{j,\ell}$ and the loss factor l_f . The shunt admittance is chosen as $B_{i,s} = 0.2$ for the two-machine system and $B_{i,s} = 0$ for the six-machine system. In both cases, the damping constant D , inertia M , relaxation time T , and internal voltage E_f are equal for each machine. They are chosen as $D = 0.2$, $M = 1$, $T = 2$, and $E_f = 1$.

nodes and the consumption of consumer nodes, thus increasing the load of the transmission lines starting from a low grid loading (i.e., small $P_1^m = -P_2^m$ or P_f).

The first machine is chosen as a *slack* that is used to balance the overall active and reactive power in the system. It serves as a reference node and its stationary phase angle and voltage are set to $\delta_1^\circ = 0$ and $E_1 = 1$, respectively. A more detailed description of how the slack is used to cover the losses and how we implemented it is given in the [Appendix](#).

Evaluating whether the corollaries agree with the linear stability analysis necessitates solving for fixed points $(\delta^\circ, \omega^\circ, E^\circ)$ given by (5). Specifically, we are looking for solutions that have a vanishing angular frequency $\omega_j^\circ = 0 \forall j$, since they correspond to solutions with the system operating at the desired reference frequency. While there are multiple possible solutions of (5) that carry no physical meaning, e.g., those having a negative voltages, we focus on one stable solution with physical meaning.

In order to find a stable state of the system, we employ a double-checking procedure. First, we solve (5) and find a fixed point using a root solver provided by Python's SciPy package⁶⁷ using the solution of the linearized equations as an initial guess. Subsequently, we perform the two-step procedure:

1. We perform a first check of the stability of the fixed point by evaluating the eigenvalue spectrum of the associated Jacobian given in (10).
2. We perform a second check of the stability of the fixed point by perturbing the fixed point by a small random disturbance and numerically solving the full equations in time domain using an appropriate fifth-order adaptive numerical solver.⁶⁸

If the fixed point found in step (1) is not linearly stable, we slightly perturb the system in step (2) forcing it to relax to a new fixed point, which we take as the final stable fixed point. This double-checking procedure, in contrast with merely employing the root-finding algorithm, ensures the fixed point that is found is stable. The subsequent analysis requires to vary the system's parameters. To ensure the system remains in a stable fixed point, we change the system's parameters in small steps (adiabatically). For sufficiently small steps, the fixed point changes only slightly and, given the system remains stable, a new fixed point can most likely be found by the root-solving algorithm when initializing the search with the previously obtained fixed point.

Having detailed the numerical procedure, we test the usefulness of the corollaries for both a lossless setting ($G_{j,\ell} = 0$) as well as for increasing losses. More precisely, we assume a fixed ratio of conductances and admittances, $G_{j,\ell} = -l_f B_{j,\ell}$, for all lines (j, ℓ) , with l_f being the loss factor. By increasing the loss factor l_f , thus increasing the resistive losses, we investigate how the bounds of stability are impacted by losses and how they compare to the numerical results, keeping in mind that the corollaries are only correct up to leading order when considering losses. For both instances, we scan over a range of different active power levels, P_1^m or P_f , and differences in reactance $\Delta X = X_j - X_j' = X - X'$, to find sets of parameters where a stable fixed point exists.

Firstly, an examination of the pure instabilities is put forward, and secondly, the mixed instability corollaries are tested.

To distinguish between different instabilities, the eigenvalues and the eigenvectors of the associated Jacobian in (10) are examined for each system in a lossless and lossy setting. As a fixed point becomes unstable, one or multiple eigenvalues pass the imaginary axis. The corresponding eigenvectors indicate which kind of instability is present and which corollary to compare to.

A. Lossless case

In the lossless case ($G_{j,\ell} = 0$), the equations of motion are considerably simplified. While different fixed points, stable and unstable, can be found, we focus on fixed points that are stable by using the aforementioned iterative procedure. In the two-machine system, the active power injected by one machine is given by P_1^m and the power extracted by the other machine is $P_2^m = -P_1^m$. In the six-machine system, the default power injection presented in [Fig. 1](#) was multiplied by the factor P_f , thus proportionally increasing the power extracted or injected at each node.

For both systems, we calculated the parameter regions where stable physically meaningful fixed points could be found using the first machine as the slack (see the [Appendix](#) for more details). By analyzing the dominant eigenvalue μ_2 of the eigenvalue spectrum of the Jacobian J , we determined where the fixed points are stable or unstable within the parameter region. By simultaneously examining the eigenvectors corresponding to the leading eigenvalue at the bifurcation point, the precise type of instability was identified. In the subsequent analysis, we will refer to the angle different between machines by the shorthand $\delta_{ij} = \delta_i - \delta_j$.

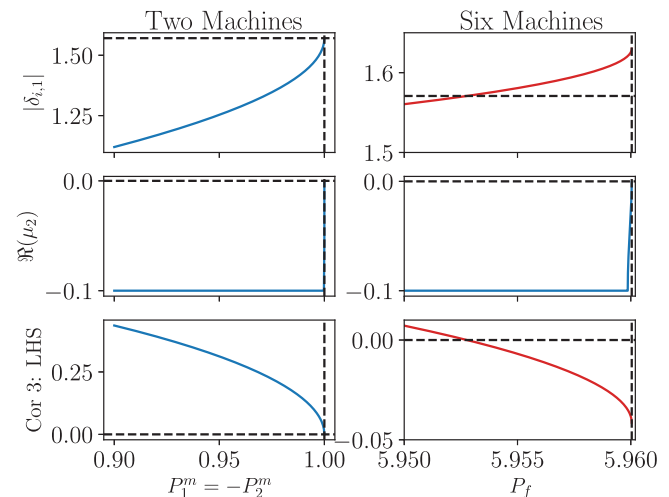


FIG. 2. Route to a pure angle instability with a difference in transient and static reactance $\Delta X = 0$ for the two-machine (left column) and six-machine system (right column). The rows show, from top to bottom, the stationary phase angle difference $|\delta_{i,1}|$, the real part of the dominant eigenvalue $\Re(\mu_2)$, and the left-hand side (LHS) of Corollary 3. The stable fixed point is lost at $P_1^m = -P_2^m = 1$ and $P_f = 5.96$ for the two- and six-machine systems, respectively. These bifurcation points are almost perfectly predicted by Corollary 3.

1. Pure instability

A pure rotor angle instability could be observed for both systems by setting the difference of static and transient reactance to $\Delta X = 0$, thus isolating the rotor angle subsystem. The instability arises after increasing the level of power injection/extraction beyond $P_1^m = -P_2^m = 1$ and $P_f \approx 5.96$ for the two-machine and the six-machine system, respectively (see Fig. 2). Corollary 3 predicts the point where the maximal phase angle difference δ_{ij} of the machines connected by a line was equal to $\pi/2$ for the two- and six-machine systems. This coincides with the point where the stability of the fixed point is lost for the two-machine system, while it is slightly below the transition for the six-machine system. This shows the efficacy of Corollary 3, as it is tight in simple systems and remains near the transition point for more complex systems.

2. Mixed instability

We now turn to the emergence of mixed instabilities which are captured by Corollaries 4, 6, and 7. To best showcase the usefulness of the corollaries, we focus on the difference of the left-hand side (LHS) and the right-hand side (RHS) in each corollary, respectively.

Firstly, we examine Corollary 4 by varying the power and comparing the eigenvalue λ_2 of the reduced Laplacian with the right-hand side of the corollary, for different values of the difference in reactance ΔX . The results are shown in Fig. 3. Corollary 4 seems to be tight in both the two-machine and six-machine systems as the stability boundary coincides with the point where λ_2 and RHS are closest. Notably, we found that Corollary 4 also gives reasonable results for larger ΔX . Even while a finite gap between λ_2 and the

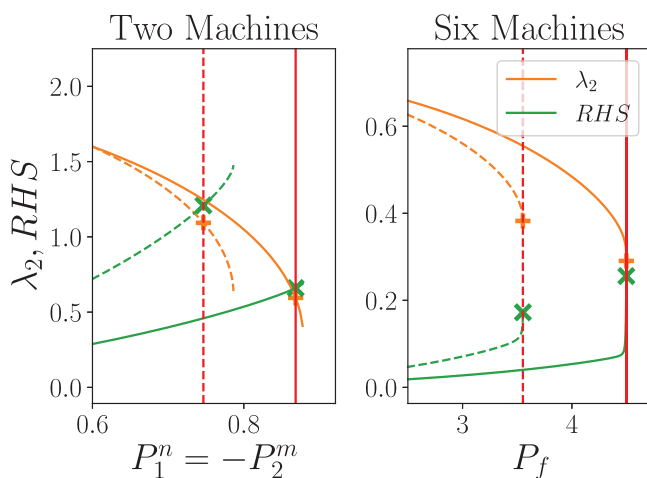


FIG. 3. Evaluation of Corollary 4 for $\Delta X = 0.2$ (solid lines) and $\Delta X = 0.5$ (dashed lines) for increasing loading of the system. The system loses stability when the dominant eigenvalue μ_2 crosses the imaginary axis, which is indicated by the red vertical lines. The values close to the transition points are highlighted with crosses for both λ_2 and the right-hand side RHS of the corollary. At this point, the dominant eigenvalues of the reduced Laplacian λ_2 and the right-hand side are closest to each other, highlighting the usefulness of Corollary 4.

RHS remains, the gradient of the difference could serve as an early warning signal for reaching the bifurcation point.

Secondly, we evaluate Corollaries 6 and 7 and show the results in Fig. 4. In the white regions, no stable fixed point can be found. Therein, we have $LHS - RHS < 0$ for both corollaries, i.e., the corollaries are not satisfied. The gray hatched region shows the case where $LHS - RHS < 0$, i.e., the corollaries are not satisfied, but there is a stable fixed point. Given these corollaries are sufficient criteria for stability, this distinction is to be expected: the failure to satisfy the corollaries is not an indication of instability; it is simply an indication that no assertions on the stability of the system can be made on the basis of these corollaries. Nevertheless, we note that Corollaries 6 and 7 are very tight for the two-machine system, proving their efficacy in determining stability. They also adequately reproduce the qualitative shape of the stability boundary for the six-machine

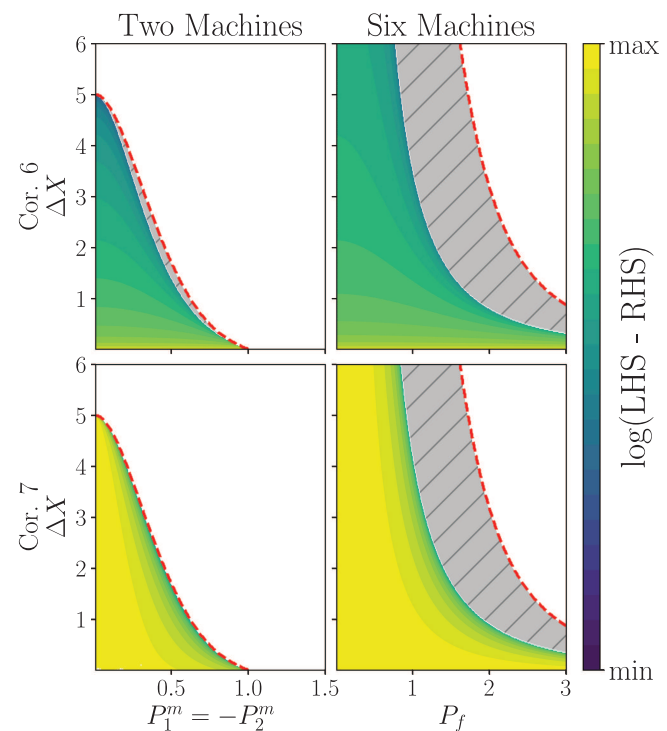


FIG. 4. Comparison of the numerically determined stability boundaries and the sufficient criteria given by Corollaries 6 and 7. The red dashed lines show the boundaries of the parameter regions for which a stable fixed point exists according to the dominant eigenvalue of the Jacobian μ_2 in both the two- and six-machine systems (cf. Fig. 1). The colormap shows the logarithm of left-hand side (LHS) minus right-hand side (RHS) of the corollaries corresponding to mixed instabilities for two machines (left column) and six machines (right column), as a function of power injection/extraction and difference in reactance. Note that only values are shown that are positive and thus the logarithm used for the color scale gives a real value. In the white region, no stable fixed points exist. Correspondingly, the sufficient criteria are not satisfied ($LHS - RHS < 0$). In the colored area $LHS - RHS > 0$ such that a stable fixed point exists according to the Corollaries 6 and 7. While the sufficient criteria are not satisfied ($LHS - RHS < 0$) in the gray hatched area, a stable fixed point still exists in this area.

system. For $\Delta X \neq 0$, only mixed instabilities could be observed for both systems.

B. Lossy case

So far, we considered solely lossless systems. We showed that the related corollaries for pure instabilities are tight and that Corollaries 4, 6, and 7 adequately describe the stability boundary (perfectly in the case of two machines). We now turn to the more interesting case where losses are included. Again, the two- and six-machine systems were considered.

Before checking the corollaries and how the results obtained by the perturbation ansatz (34) compared to numerical results, we have to find the correct fixed point. Power losses on the transmission lines are not known *a priori* before the fixed point is determined. Hence, we use the slack node $j = 1$ to ensure that the power is balanced assuming that it includes an appropriate control system. Technically, we suspend the power balance equation and the voltage equation in (5) and set $\delta_1^o = 0$ and $E_1^o = 1$ during the root-solving procedure. Afterward, we set P_1^m and E_1^f to satisfy (5).

If losses were considered, only mixed instability could be observed. Therefore, the corollaries corresponding to mixed instabilities were evaluated and are shown in Figs. 5 and 6.

Firstly, we examine the usefulness of Corollary 4 in Fig. 5. We again observe that the point where stability is lost coincides with the point where the eigenvalue λ_2 and the right-hand side of the corollary are closest. Note that it becomes numerically hard to determine the exact point where $\Re(\mu_2) = 0$ for the case with high losses and small ΔX . Nevertheless, the corollary works well at intermediate values for ΔX , although having been designed up to leading order in

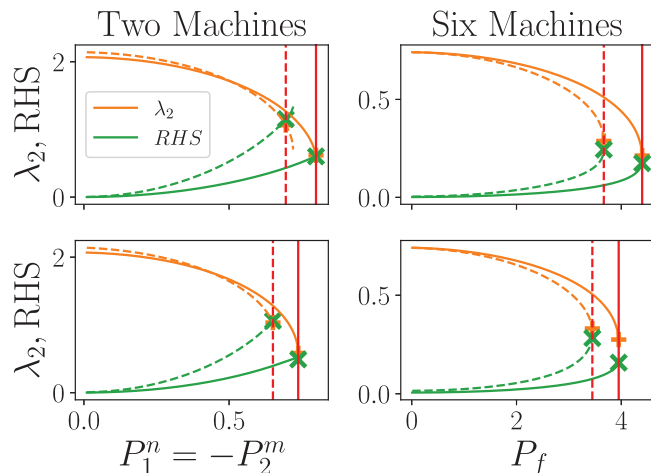


FIG. 5. Evaluation of Corollary 4 for different ΔX and loss factors. The point where stability is lost is indicated by the horizontal red lines. The loss factors were chosen as $l_f = 0.1$ and $l_f = 0.2$ in the top and bottom row, respectively. The solid lines show the results for $\Delta X = 0.2$, whereas the dashed lines show the results for $\Delta X = 0.5$. While it is numerically challenging to determine the point where stability is lost (i.e., $\mu_2 = 0$) for low ΔX and non-zero loss factors l_f , Corollary 4 adequately predicts the bifurcation points for the considered systems, ΔX and l_f .

ΔX , serving well at these ranges as an early warning for imminent instability.

Secondly, we examine Corollaries 6 and 7 and show the related results in Fig. 6. The colored areas show the region where Corollaries 6 and 7 are satisfied. These do not fully cover the parameter region with a linearly stable fixed point as the loss factor l_f increases. Additionally, the approximation $\Delta X \approx 0$ used to find the Fiedler vector in Corollary 7 limits the range of ΔX where the corollaries are insightful in the sense of overlapping with the area of a stable fixed point given by the dominant eigenvalues. Overall, the sufficient stability conditions remain correct for all values of l_f although they were derived solely to leading order in the losses. That is, at every point in parameter space where 6 and 7 imply the fixed point is stable agrees with the real part of the dominant non-zero eigenvalue of the corresponding Jacobian being smaller than zero.

In conclusion, the developed corollaries can be used to efficiently judge whether a system's fixed point is stable without the need to calculate the full Jacobian or run simulations. This is especially useful to system operators that need to check the stability of different grid situations, since they can use the corollaries to focus on the cases where the corollaries do not indicate a stable fixed point, potentially cutting down on the amount of costly (numerical) simulations of the full dynamics.

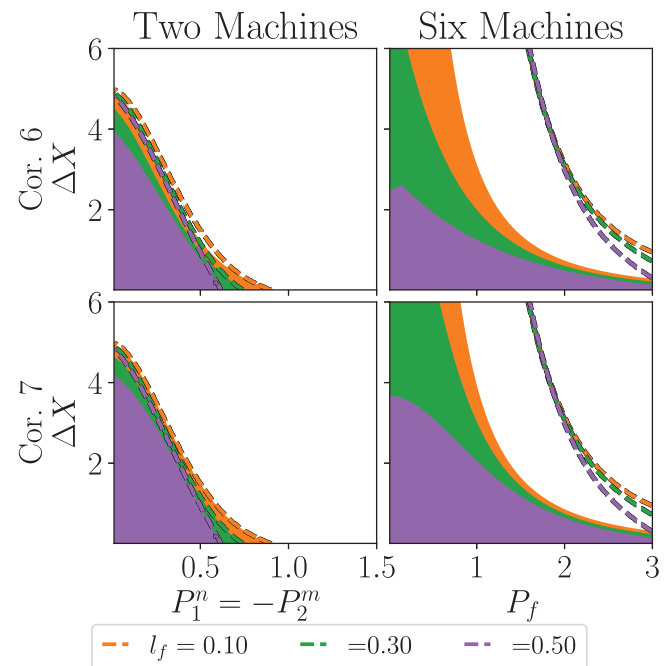


FIG. 6. Corollaries for mixed instabilities for different levels of losses in the two-machine (left column) and six-machine systems (right column). Different colors indicate different loss factors l_f according to the legend below the plot. Dashed lines show where the dominant non-zero eigenvalue μ_2 crossed the imaginary axis and the system becomes unstable. The white regions indicate the parameter region where no physically meaningful stable fixed point exists. Increasing losses by choosing a larger loss factor l_f decreases the size of the parameter region where a stable fixed point can be found.

VII. CONCLUSION

The third-order model describes the dynamics of synchronous machines and takes into account both the rotor angle and the voltage dynamics. Analytical results for the dynamics and the stability of coupled machines in power grids with complex topologies are rare, in particular, if Ohmic losses are taken into account. In this article, a comprehensive linear stability analysis was carried out and several explicit stability criteria were derived.

The first main result of this work depicts the influence of resistive terms of the system after linear stability analysis. Remarkably, these terms enter into the reduced system Jacobian only via the two diagonal matrices Γ^d and N , as shown in (28) up to leading order in the losses. As a second main result, a decomposition of the Jacobian into the rotor angle and the voltage subsystems is derived in Lemma 4, where losses are incorporated up to linear order via perturbation theory. This decomposition reveals clearly how the interplay of both subsystems can lead to mixed forms of instability and thus requires additional security margins.

Based on this decomposition, several explicit stability conditions were derived, both for the isolated subsystems as well as for the full systems, including rotor angle and voltage dynamics. In particular, one can show that the stability of the voltage system is not affected directly by resistive terms up to leading order in the losses, thus implying that studies on the stability of the voltage system withstand in the purely lossless case. Furthermore, Corollaries 4 and 5 entail a strict minimum connectivity of the power grid network solely by the presence of resistive terms, i.e., a lower bound to possible dynamics on the system given the presence of losses in the system.

The analytical insights unveiled here—especially the mathematical evaluation of lossy systems—can prove relevant to further understand power grids of all spatial scales and of general graph constructions. Notably, we have shown how the derived stability criteria are modified to linear order in the presence of Ohmic losses. This approach is particularly useful in the qualitative analysis of the stability phase diagrams and the bifurcations: Do losses lead to an increase or decrease of stable parameter regions?

In the future, our analysis may contribute to the derivation of rigorous quantitative stability conditions for lossy power grids. Moreover, it opens the door to further research on higher-order models from a mathematical point-of-view and can, henceforth, be applied more generally to other power grid models.

ACKNOWLEDGMENTS

We thank Christopher Kaschny for helpful discussions. Furthermore, we would like to thank the reviewers for their thorough work that improved the quality of the original manuscript significantly. We gratefully acknowledge support from the German Federal Ministry of Education and Research (Grant No. 03EK3055B), the German Federal Ministry for Economic Affairs and Energy (BMWi) via the project DYNAMOS (Grant No. 03ET4027A), and the Helmholtz Association via the grant *Uncertainty Quantification—From Data to Reliable Knowledge* (UQ) (Grant No. ZT-I-0029). This study was also funded by the Deutsche Forschungsgemeinschaft (DFG, German Research Foundation, Grant No. 491111487).

AUTHOR DECLARATIONS

Conflict of Interest

The authors have no conflicts to disclose.

DATA AVAILABILITY

The data that support the findings of this study are available from the corresponding author upon reasonable request.

APPENDIX: EXISTENCE OF SOLUTIONS FOR TWO MACHINES

In this Appendix, we provide more details on the existence of fixed points for the two-machine system, i.e., the solution of the algebraic (5) for $N = 2$. In particular, we discuss how the choice of E_j^f affects the stability of the system.

So assume that machine 1 acts as an effective generator ($P_1^m > 0$) and machine 2 acts as an effective motor ($P_2^m < 0$). We use P_2^m as an external parameter to vary the loading of the grid. The generator has to cover the load of the motor as well as the losses, hence we cannot fix P_1^m beforehand. Instead, it is assumed that P_1^m is set by a control system to guarantee a balanced system, $\Omega = 0$. From a computational viewpoint, node 1 is treated as a slack and the power injection is computed as a function of the free system variables via

$$P_1^m = G_{1,1}E_1^2 + E_1^2E_2^2 [B_{1,2} \sin(\delta_{1,2}^\circ) + G_{1,2} \cos(\delta_{1,2}^\circ)], \quad (A1)$$

using the abbreviation $\delta_{1,2}^\circ = \delta_1^\circ - \delta_2^\circ$. We further assume that the remaining machine parameters are equal, $X_1 - X_1' = X_2 - X_2' = \Delta X$, $B_{1,1} = B_{2,2}$, $G_{1,1} = G_{2,2}$, $B_{1,2} = B_{2,1}$, and $G_{1,2} = G_{2,1}$. We now distinguish three cases with respect to the choice of the field flux E_j^f .

(a) We first consider the case that *both* machines are equipped with a control system that sets the actual voltages at a predefined set value, which we set to unity in appropriate units, i.e., $E_1^\circ = E_2^\circ = 1$. To achieve this, the field fluxes have to be set to

$$E_1^f = 1 - \Delta X [B_{1,1} + B_{1,2} \cos(\delta_{1,2}^\circ) - G_{1,2} \sin(\delta_{1,2}^\circ)] \quad (A2)$$

$$E_2^f = 1 - \Delta X [B_{2,2} + B_{1,2} \cos(\delta_{2,1}^\circ) - G_{1,2} \sin(\delta_{2,1}^\circ)]. \quad (A3)$$

The only remaining unknown state variable is the phase difference $\delta_{2,1}^\circ = \delta_2^\circ - \delta_1^\circ = -\delta_{1,2}^\circ$ between the two nodes, which is obtained from the power balance equation,

$$\begin{aligned} P_2^m &= G_{2,2} + B_{1,2} \sin(\delta_{2,1}^\circ) + G_{1,2} \cos(\delta_{2,1}^\circ) \\ &= G_{2,2} + |Y_{1,2}| \sin(\delta_{2,1}^\circ - \gamma_{1,2}), \end{aligned} \quad (A4)$$

where we have defined $|Y_{1,2}| = \sqrt{B_{1,2}^2 + G_{1,2}^2}$ and

$$B_{1,2} = |Y_{1,2}| \cos(\gamma_{1,2}), \quad \text{and} \quad G_{1,2} = -|Y_{1,2}| \sin(\gamma_{1,2}). \quad (A5)$$

Solving the power imbalance then yields

$$\delta_{2,1}^\circ = \gamma_{1,2} + \arcsin\left(\frac{P_2^m - G_{2,2}}{|Y_{1,2}|}\right) \quad (A6)$$

or

$$\delta_{2,1}^\circ = \gamma_{1,2} - \arcsin\left(\frac{P_2^m - G_{2,2}}{|Y_{1,2}|}\right) + \pi. \quad (\text{A7})$$

We thus obtain two fixed points if

$$|P_2^m - G_{2,2}| \leq |Y_{1,2}|, \quad (\text{A8})$$

which coalesce in case of equality. The dynamical stability of these two solutions is then checked by computing the eigenvalues of the Jacobian. If the condition (A8) is not satisfied, no fixed point exists.

(b) Second, we may assume that only the generator or slack node is equipped with a control system which fixes $E_1^\circ = 1$, whereas E_2° is a state variable that is yet to be determined. The field flux E_1^f is still given by

$$E_1^f = 1 - \Delta X [B_{1,1} + E_2^\circ (B_{1,2} \cos(\delta_{1,2}^\circ) - G_{1,2} \sin(\delta_{1,2}^\circ))], \quad (\text{A9})$$

while E_2^f is a fixed machine parameter. The power balance equation at node 2 yields $\delta_{1,2}^\circ$ in terms of E_2°

$$\sin(\delta_{2,1}^\circ - \gamma_{1,2}) = \frac{P_2^m - G_{2,2} E_2^{\circ 2}}{|Y_{1,2}| E_2^\circ}. \quad (\text{A10})$$

Now we can use (5) to obtain E_2° . We have

$$0 = E_2^f - E_2^\circ + \Delta X B_{2,2} E_2^\circ + \Delta X |Y_{1,2}| \cos(\delta_{2,1}^\circ - \gamma_{1,2}). \quad (\text{A11})$$

Squaring this equation and using $\cos^2 = 1 - \sin^2$ then yields

$$\begin{aligned} & \left[(1 - \Delta X B_{2,2}) E_2^\circ - E_2^f \right]^2 E_2^{\circ 2} \\ &= \Delta X^2 |Y_{1,2}| E_2^{\circ 2} - \Delta X^2 [P_2^m - G_{2,2} E_2^{\circ 2}]^2. \end{aligned} \quad (\text{A12})$$

This is a fourth-order polynomial in E_2° , which can be solved in a straightforward way. The exact solutions are quite lengthy and are not given here. However, we remark that one can obtain conditions for the existence of physical solution, i.e., solutions where E_2° is real and non-negative. We can then check the dynamical stability of the physical solutions by computing the eigenvalues of the Jacobian.

(c) Finally, we are left with the case where no machine has a control system. That is, both E_1^f and E_2^f are fixed system parameters and E_1° and E_2° are free system parameters that are yet to be determined. In the general case, we cannot obtain an analytical solution and thus have to resort to numerical computations.

In the case of a lossless line and identical machines ($E_1^f = E_2^f = E^f$), however, we can obtain such a solution. The fixed point (5) now yield

$$0 = E^f - E_2^\circ + \Delta X B_{1,1} E_2^\circ + \Delta X B_{1,2} E_1^\circ \cos(\delta_{2,1}^\circ), \quad (\text{A13})$$

$$0 = E^f - E_1^\circ + \Delta X B_{1,1} E_1^\circ + \Delta X B_{1,2} E_2^\circ \cos(\delta_{2,1}^\circ). \quad (\text{A14})$$

Multiplying the equations with E_1° and E_2° , respectively, and subtracting the resulting equations yields

$$0 = E^f (E_2^\circ - E_1^\circ) - (1 - \Delta X B_{1,1}) (E_2^{\circ 2} - E_1^{\circ 2}) \quad (\text{A15})$$

$$= (E_2^\circ - E_1^\circ) [E^f - (1 - \Delta X B_{1,1}) (E_2^\circ + E_1^\circ)]. \quad (\text{A16})$$

This condition requires that one of the brackets vanishes. One can show that the expression in the square bracket is always non-zero,

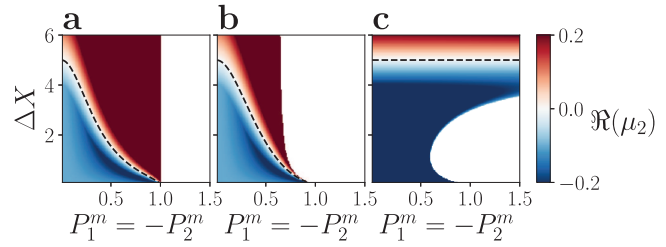


FIG. 7. Stability map of a lossless system with two machines and different slack implementations. The figure shows the existence of a fixed point and the dominant eigenvalue $\Re(\mu_2)$ as a function of the grid load $P_1^m = -P_2^m$ and the machine parameter ΔX . The three panels show three different scenarios for the control of the field fluxes E_f^f . (a) Both machines have a control system that adapts E_1^f and E_2^f such that the voltages assume a predefined value which is set to unity, $E_1^f = E_2^f = 1$. (b) Only the effective generator or slack node has a control system fixing $E_1^f = 1$ while the other node has a fixed $E_2^f = 1$. (c) Both machines have a fixed value for the field flux $E_1^f = E_2^f = 1$. The regions of stability are visible for different definitions of a slack and/or control system. The dashed black line indicates where the dominant eigenvalue crosses the imaginary axis and the considered fixed point becomes unstable. No fixed points exist in the white regions.

hence the only possible solution is given by $E_2^\circ = E_1^\circ$. The remaining equations to solve are then given by

$$P_2^m = B_{1,2} E_1^{\circ 2} \sin(\delta_{2,1}^\circ), \quad (\text{A17})$$

$$E_1^\circ (1 - \Delta X B_{1,1}) = E^f + \Delta X B_{1,2} E_1^\circ \cos(\delta_{2,1}^\circ). \quad (\text{A18})$$

Using the first equation to eliminate the cosine from the second equation yields

$$[E_1^\circ (1 - \Delta X B_{1,1}) - E^f]^2 E_1^{\circ 2} = \Delta X^2 B_{1,2}^2 E_1^{\circ 4} - \Delta X^2 (P_2^m)^2.$$

This is again a fourth-order polynomial in E_1° , which can be solved in a straightforward way.

A stability map for the three different cases is provided in Fig. 7. Stability properties are similar for small values of ΔX but differ significantly for larger values. In the main body of the manuscript, we focus on the case (b) to test the significance and tightness of the derived stability conditions.

REFERENCES

- ¹R. Sims *et al.*, "Integration of renewable energy into present and future energy systems," in *IPCC Special Report on Renewable Energy Sources and Climate Change Mitigation*, edited by O. Edenhofer *et al.* (Cambridge University Press, Cambridge, 2011), pp. 609–706.
- ²F. Milano, F. Dörfler, G. Hug, D. J. Hill, and G. Verbič, "Foundations and challenges of low-inertia systems (invited paper)," in *2018 Power Systems Computation Conference (PSCC)* (IEEE, 2018), pp. 1–25.
- ³B. Schäfer, D. Witthaut, M. Timme, and V. Latora, "Dynamically induced cascading failures in power grids," *Nat. Commun.* **9**, 378 (2018).
- ⁴H. Taher, S. Olmi, and E. Schöll, "Enhancing power grid synchronization and stability through time-delayed feedback control," *Phys. Rev. E* **100**, 062306 (2019).
- ⁵Ph. C. Böttcher, A. Otto, S. Kettemann, and C. Agert, "Time delay effects in the control of synchronous electricity grids," *Chaos* **30**, 013122 (2020).

- ⁶U. Markovic, O. Stanojev, P. Aristidou, E. Vrettos, D. Callaway, and G. Hug, "Understanding small-signal stability of low-inertia systems," *IEEE Trans. Power Syst.* **36**, 3997–4017 (2021).
- ⁷W. J. Farmer and A. J. Rix, "Impact of continuous stochastic and spatially distributed perturbations on power system frequency stability," *Electr. Power Syst. Res.* **201**, 107536 (2021).
- ⁸W. J. Farmer and A. J. Rix, "Analysing the power system frequency dynamics subject to continuous spatial-temporal fluctuations," in *2021 4th Asia Conference on Energy and Electrical Engineering (ACEEE)* (IEEE, 2021), pp. 24–28.
- ⁹L. Rydin Gorjão, B. Schäfer, D. Witthaut, and C. Beck, "Spatio-temporal complexity of power-grid frequency fluctuations," *New J. Phys.* **23**, 073016 (2021).
- ¹⁰J. Machowski, Z. Lubosny, J. W. Bialek, and J. R. Bumby, *Power System Dynamics: Stability and Control*, 3rd ed. (John Wiley & Sons, New York, 2020).
- ¹¹R. H. Lasseter and P. Piagi, "Microgrid: A conceptual solution," in *IEEE Power Electronics Specialists Conference* (IEEE, 2004), Vol. 6, pp. 4285–4291.
- ¹²J. Rocabert, A. Luna, F. Blaabjerg, and P. Rodriguez, "Control of power converters in AC microgrids," *IEEE Trans. Power Electron.* **27**, 4734–4749 (2012).
- ¹³F. Guo, C. Wen, and Y.-D. Song, *Distributed Control and Optimization Technologies in Smart Grid Systems*, 1st ed. (CRC Press, Boca Raton, FL, 2017), p. 214.
- ¹⁴U. B. Tayab, M. A. B. Roslan, L. J. Hwai, and M. Kashif, "A review of droop control techniques for microgrid," *Renew. Sust. Energ. Rev.* **76**, 717–727 (2017).
- ¹⁵F. Dörfler, S. Bolognani, J. W. Simpson-Porco, and S. Grammatico, "Distributed control and optimization for autonomous power grids," in *2019 18th European Control Conference (ECC)* (IEEE, 2019), pp. 2436–2453.
- ¹⁶M. Rohden, A. Sorge, D. Witthaut, and M. Timme, "Impact of network topology on synchrony of oscillatory power grids," *Chaos* **24**, 013123 (2014).
- ¹⁷M. Farokhian Firuzi, A. Roosta, and M. Gitizadeh, "Stability analysis and decentralized control of inverter-based AC microgrid," *Prot. Control Mod. Power Syst.* **4**, 78 (2019).
- ¹⁸T. Coletta and P. Jacquod, "Linear stability and the Braess paradox in coupled-oscillator networks and electric power grids," *Phys. Rev. E* **93**, 032222 (2016).
- ¹⁹L. Pagnier and Ph. Jacquod, "Optimal placement of inertia and primary control: A matrix perturbation theory approach," *IEEE Access* **7**, 145889–145900 (2019).
- ²⁰L. Tumash, S. Olmi, and E. Schöll, "Stability and control of power grids with diluted network topology," *Chaos* **29**, 123105 (2019).
- ²¹M. Tyloo and Ph. Jacquod, "Primary control effort under fluctuating power generation in realistic high-voltage power networks," *IEEE Control Syst. Lett.* **5**, 929–934 (2021).
- ²²M. Tyloo and Ph. Jacquod, "Global robustness versus local vulnerabilities in complex synchronous networks," *Phys. Rev. E* **100**, 032303 (2019).
- ²³F. Hellmann, P. Schultz, P. Jaros, R. Levchenko, T. Kapitaniak, J. Kurths, and Y. Maistrenko, "Network-induced multistability through lossy coupling and exotic solitary states," *Nat. Commun.* **11**, 2005 (2020).
- ²⁴M. Thümler, X. Zhang, and M. Timme, [arXiv:2111.15590](https://arxiv.org/abs/2111.15590) (2021).
- ²⁵M. He, W. He, J. Hu, X. Yuan, and M. Zhan, "Nonlinear analysis of a simple amplitude-phase motion equation for power-electronics-based power system," *Nonlinear Dyn.* **95**, 1965–1976 (2019).
- ²⁶Q. Qiu, R. Ma, J. Kurths, and M. Zhan, "Swing equation in power systems: Approximate analytical solution and bifurcation curve estimate," *Chaos* **30**, 013110 (2020).
- ²⁷J. Schiffer, R. Ortega, A. Astolfi, J. Raisch, and T. Sezi, "Conditions for stability of droop-controlled inverter-based microgrids," *Automatica* **50**, 2457–2469 (2014).
- ²⁸J. Schiffer, T. Seel, J. Raisch, and T. Sezi, "Voltage stability and reactive power sharing in inverter-based microgrids with consensus-based distributed voltage control," *IEEE Trans. Control Syst. Technol.* **24**, 96–109 (2016).
- ²⁹J. Schiffer, F. Dörfler, and E. Fridman, "Robustness of distributed averaging control in power systems: Time delays & dynamic communication topology," *Automatica* **80**, 261–271 (2017).
- ³⁰F. Dörfler and F. Bullo, "Synchronization and transient stability in power networks and non-uniform Kuramoto oscillators," *SIAM J. Control Optim.* **50**, 1616–1642 (2012).
- ³¹F. Dörfler, M. Chertkov, and F. Bullo, "Synchronization in complex oscillator networks and smart grids," *Proc. Natl. Acad. Sci. U.S.A.* **110**, 2005–2010 (2013).
- ³²P. C. Krause, O. Wasynczuk, S. D. Sudhoff, and S. Pekarek, *Analysis of Electric Machinery and Drive Systems*, 3rd ed. (Wiley Online Library, 2013).
- ³³P. W. Sauer, M. A. Pai, and J. H. Chow, *Power System Dynamics and Stability: With Synchrophasor Measurement and Power System Toolbox*, 2nd ed. (Prentice Hall, Upper Saddle River, NJ, 2017).
- ³⁴K. Schmietendorf, J. Peinke, R. Friedrich, and O. Kamps, "Self-organized synchronization and voltage stability in networks of synchronous machines," *Eur. Phys. J. Spec. Top.* **223**, 2577–2592 (2014).
- ³⁵S. Auer, K. Kleis, P. Schultz, J. Kurths, and F. Hellmann, "The impact of model detail on power grid resilience measures," *Eur. Phys. J. Spec. Top.* **225**, 609–625 (2016).
- ³⁶K. Schmietendorf, J. Peinke, and O. Kamps, [arXiv:1611.08235](https://arxiv.org/abs/1611.08235) (2016).
- ³⁷B. J. Pierre, H. N. Villegas Pico, R. T. Elliott, J. Flicker, Y. Lin, B. B. Johnson, J. H. Eto, R. H. Lasseter, and A. Ellis, "Bulk power system dynamics with varying levels of synchronous generators and grid-forming power inverters," in *2019 IEEE 46th Photovoltaic Specialists Conference (PVSC)* (IEEE, 2019), pp. 0880–0886.
- ³⁸L. Wu and H. Chen, "Synchronization conditions for a third-order Kuramoto network," in *2020 59th IEEE Conference on Decision and Control (CDC)* (IEEE, 2020), pp. 5834–5839.
- ³⁹K. S. Suchithra, E. A. Gopalakrishnan, E. Surovyatkina, and J. Kurths, "Rate-induced transitions and advanced takeoff in power systems," *Chaos* **30**, 061103 (2020).
- ⁴⁰W. Huang and D. J. Hill, "Network-based analysis of long-term voltage stability considering loads with recovery dynamics," *Int. J. Electr. Power Energy Syst.* **119**, 105891 (2020).
- ⁴¹W. Yi and D. J. Hill, "Topological stability analysis of high renewable penetrated systems using graph metrics," in *2021 IEEE Madrid PowerTech* (IEEE, 2021), pp. 1–6.
- ⁴²K. Sharafutdinov, L. Rydin Gorjão, M. Matthiae, T. Faulwasser, and D. Witthaut, "Rotor-angle versus voltage instability in the third-order model for synchronous generators," *Chaos* **28**, 033117 (2018).
- ⁴³T. Weckesser, H. Jóhannsson, and J. Østergaard, "Impact of model detail of synchronous machines on real-time transient stability assessment," in *2013 IREP Symposium Bulk Power System Dynamics and Control-IX Optimization, Security and Control of the Emerging Power Grid* (IEEE, 2013), pp. 1–9.
- ⁴⁴G. Kron, *Tensor Analysis of Networks*, 1st ed. (J. Wiley & Sons, New York, 1939).
- ⁴⁵F. Dörfler and F. Bullo, "Kron reduction of graphs with applications to electrical networks," *IEEE Trans. Circuits Syst. I Regul. Pap.* **60**, 150–163 (2013).
- ⁴⁶J. Ma, Y. Sun, X. Yuan, J. Kurths, and M. Zhan, "Dynamics and collapse in a power system model with voltage variation: The damping effect," *PLoS ONE* **11**, e0165943 (2016).
- ⁴⁷A. J. Korsak, "On the question of uniqueness of stable load-flow solutions," *IEEE Trans. Power Apparatus Syst.* **PAS-91**, 1093–1100 (1972).
- ⁴⁸R. Delabays, T. Coletta, and Ph. Jacquod, "Multistability of phase-locking and topological winding numbers in locally coupled Kuramoto models on single-loop networks," *J. Math. Phys.* **57**, 032701 (2016).
- ⁴⁹D. Manik, M. Timme, and D. Witthaut, "Cycle flows and multistability in oscillatory networks," *Chaos* **27**, 083123 (2017).
- ⁵⁰S. Jafarpour, E. Y. Huang, K. D. Smith, and F. Bullo, [arXiv:1901.11189](https://arxiv.org/abs/1901.11189) (2019).
- ⁵¹R. E. Mirollo and S. H. Strogatz, "The spectrum of the locked state for the Kuramoto model of coupled oscillators," *Physica D* **205**, 249–266 (2005).
- ⁵²S. H. Strogatz, *Nonlinear Dynamics and Chaos: With Applications to Physics, Biology, Chemistry, and Engineering*, 2nd ed. (CRC Press, Boca Raton, FL, 2015).
- ⁵³Y. A. Kuznetsov, *Elements of Applied Bifurcation Theory*, 3rd ed. (Springer-Verlag, New York, 2004), Vol. 112.
- ⁵⁴F. Zhang, *The Schur Complement and its Applications*, 1st ed. (Springer Science & Business Media, 2006), Vol. 4.
- ⁵⁵D. Manik, D. Witthaut, B. Schäfer, M. Matthiae, A. Sorge, M. Rohden, E. Kati-fori, and M. Timme, "Supply networks: Instabilities without overload," *Eur. Phys. J. Spec. Top.* **223**, 2527 (2014).
- ⁵⁶D. Zelazo and M. Bürger, "On the definiteness of the weighted Laplacian and its connection to effective resistance," in *53rd IEEE Conference on Decision and Control* (IEEE, 2014), pp. 2895–2900.
- ⁵⁷Y. Song, D. J. Hill, and T. Liu, "Small-disturbance angle stability analysis of microgrids: A graph theory viewpoint," in *IEEE International Conference on Control Applications (CCA)* (IEEE, 2015), pp. 201–206.

- ⁵⁸W. Chen, D. Wang, J. Liu, T. Basar, K. H. Johansson, and L. Qiu, "On semidefiniteness of signed Laplacians with application to microgrids," *IFAC-PapersOnLine* **49–22**, 97–102 (2016).
- ⁵⁹W. Chen, J. Liu, Y. Chen, S. Z. Khong, D. Wang, T. Basar, L. Qiu, and K. H. Johansson, "Characterizing the positive semidefiniteness of signed Laplacians via effective resistances," in *55th IEEE Conference on Decision and Control (CDC)* (IEEE, 2016), pp. 985–990.
- ⁶⁰S. Geršgorin, "Über die abgrenzung der eigenwerte einer Matrix," *Izv. Akad. Nauk S.S.S.R. Otd. Mat. Estestvennykh Nauk* **6**, 749–754 (1931).
- ⁶¹M. Newman, *Networks: An Introduction*, 2nd ed. (Oxford University Press, 2018).
- ⁶²M. Fiedler, "Algebraic connectivity of graphs," *Czech. Math. J.* **23**, 298 (1973).
- ⁶³M. Fiedler, "A property of eigenvectors of nonnegative symmetric matrices and its application to graph theory," *Czech. Math. J.* **25**, 619–633 (1975).
- ⁶⁴F. R. K. Chung and F. C. Graham, *Spectral Graph Theory*, 1st ed. (American Mathematical Society, 1997), Vol. 92.
- ⁶⁵G. Filatrella, A. H. Nielsen, and N. F. Pedersen, "Analysis of a power grid using a Kuramoto-like model," *Eur. Phys. J. B* **61**, 485–491 (2008).
- ⁶⁶T. Nishikawa and A. E. Motter, "Comparative analysis of existing models for power-grid synchronization," *New J. Phys.* **17**, 015012 (2015).
- ⁶⁷P. Virtanen, R. Gommers, T. E. Oliphant, M. Haberland, T. Reddy, D. Cournapeau, E. Burovski, P. Peterson, W. Weckesser, J. Bright, S. J. van der Walt, M. Brett, J. Wilson, K. Jarrod Millman, N. Mayorov, A. R. J. Nelson, E. Jones, R. Kern, E. Larson, C. Carey, Í. Polat, Y. Feng, E. W. Moore, J. VanderPlas, D. Laxalde, J. Perktold, R. Cimrman, I. Henriksen, E. A. Quintero, C. R. Harris, A. M. Archibald, A. H. Ribeiro, F. Pedregosa, P. van Mulbregt, and Contributors, "SciPy 1.0: Fundamental algorithms for scientific computing in python," *Nat. Methods* **17**, 261–272 (2020).
- ⁶⁸G. Ansmann, "Efficiently and easily integrating differential equations with JiTCODE, JiTCDDE, and JiTCSDE," *Chaos* **28**, 043116 (2018).